

### DOTTORATO DI RICERCA IN SCIENZE BIOMEDICHE E NEUROMOTORIE

Ciclo 37

**Settore Concorsuale:** 06/A4 - ANATOMIA PATOLOGICA

Settore Scientifico Disciplinare: MED/08 - ANATOMIA PATOLOGICA

### BRAFV600E-MUTATED COLORECTAL CANCER: PRIMARY AND ACQUIRED RESISTANCE TO TARGETED TREATMENT (MASCARA STUDY)

Presentata da: Francesca Rebuzzi

Coordinatore Dottorato Supervisore

Matilde Yung Follo Paola Ulivi

**Co-supervisore** 

Giovanna Cenacchi

#### **INDEX**

1.	INTRODUCTION  1.1 COLORECTAL CANCER (CRC)			
	1.1.1 Epidemiology			
	1.1.2	Etiology and risk factors	2	
	1.1.3	Screening, surveillance and diagnosis of CRC	3	
	1.1.4	Molecular pathogenesis of CRC	6	
	1.1.5	Consensus Molecular Subtypes (CMSs) of CRC	8	
	1.1.6	Staging of CRC	10	
	1.1.7	Treatment and follow-up of CRC	12	
	1.1.8	Liquid biopsy in CRC	17	
	1.2 <i>BRAFV60</i>	$00E$ -MUTATED METASTATIC COLORECTAL CANCER (BRAF $^{ m V600}$	)Emut	
	mCRC)		20	
	1.2.1	BRAF gene: Mechanisms, Mutations, and Implications in CRCs	20	
	1.2.2	Clinical-pathological and molecular features of $BRAF^{V600Emut}$ mCRC	22	
	1.2.3	Management of BRAF <sup>V600Emut</sup> mCRC	24	
2.	AIMS		27	
3.	PATIENTS ANI	D METHODS	28	
	3.1 BRAF-V6	600E-Mutated colorectal cAncer: primary and acquired resistance		
	to tArgetedtReAtment (MASCARA project)			
	3.2 Patient en	rollment	28	
	3.3 DNA isola	ation from Formalin-Fixed Paraffin-Embedded (FFPE) tissue samples	29	
	3.4 Whole Ex	come Sequencing (WES)	30	
	3.5 Circulatin	g tumor DNA (ctDNA) isolation from plasma samples	31	
	3.6 TruSight <sup>T</sup>	M Oncology 500 ctDNA	32	
	3.7 NanoStrir	ng GeoMx® Digital Spatial Profiler	33	
	3.8 Bioinform	natical analysis	34	
4.	RESULTS		37	
	4.1 Patient ch	aracteristics	38	
	4.2 WES data	analysis	38	
	4.3 Liquid bio	ppsy data analysis	41	
	4.4 Spatial tra	nnscriptomic preliminary analysis	44	
5.	DISCUSSION		48	
6.	<b>FUTURE PERS</b>	PECTIVES	54	

7.	REFERENCES	55
8.	ACKNOWLEDGMENTS	64

#### **ABSTRACT**

BRAF-mutant metastatic colorectal cancer (mCRC) is a highly aggressive subtype with poor prognosis and limited therapeutic options. The BRAFV600E mutation, present in 10% of CRC cases, is linked to rapid disease progression and resistance to standard treatments. Although combination therapies like Encorafenib and Cetuximab have shown promise, identifying reliable predictive biomarkers remains a challenge. The MASCARA study aims to explore the clinical and molecular features of BRAF-mutant mCRC and identify biomarkers for predicting treatment response. A cohort of 50 patients, with 30 analyzed for clinical data and genomic profiles, is being studied using whole exome sequencing (WES), liquid biopsy (ctDNA), and spatial transcriptomics to map the genetic and molecular landscape of this cancer subtype.

Initial results revealed a median patient age of 69, with a predominance of female patients (70%) and tumors primarily located in the right colon (80%). Metastases were mainly in the liver (40%) and lungs (30%). Treatment response, assessed by RECIST criteria, showed that 20% of patients had a complete or partial response to Encorafenib and Cetuximab, while 80% were non-responders. Genomic analysis confirmed the *BRAFV600E* mutation in all patients, along with frequent mutations in *TP53*, *BRINP3*, and other key genes. Notably, 80% of patients were microsatellite stable (MSS) and 87% exhibited a high tumor mutational burden (TMB-H). Mutations in *NOTCH3*, *LRP2*, and *FBXW7* were linked to resistance mechanisms, with *NOTCH3* implicated in chemotherapy resistance by modulating survival and immune pathways.

Liquid biopsy analysis revealed mutations in RAS, BRAF, PIK3CA, and SMAD4, highlighting the role of clonal evolution and activation of survival pathways in acquired resistance. Spatial transcriptomics identified differences in immune-related gene expression between responders and non-responders. Responders exhibited upregulation of immune activation pathways, such as enhanced antigen presentation and increased expression of genes like CD74, HLA-DRA, and HLA-DRB, which are integral to the immune system's ability to recognize and target tumor cells. This indicates a more immune-permissive tumor microenvironment (TME) in responders, where immune cells likely play a critical role in controlling tumor growth. In contrast, non-responders showed a predominantly immune-suppressive microenvironment, with upregulation of immune evasion genes such as SSX1 and CCL15, and downregulation of key tumor-suppressive genes like ACTB and EPCAM. These alterations suggest a TME more conducive to tumor survival and resistance to therapy, where the immune system's ability to attack the cancer cells is compromised.

Pathway analysis revealed that responders had enrichment in immune-related pathways, including antigen presentation (p = 0.007) and cytoprotection (p = 0.008), suggesting an active immune system capable of tumor recognition and immune surveillance. In contrast, non-responders exhibited

enrichment in survival and immune evasion pathways, such as FGFR2 cascade activation (p = 0.007) and GPCR receptor activation (p = 0.01), supporting tumor immune evasion and resistance to treatment.

These findings underscore the importance of both genetic alterations and immune microenvironment features in predicting treatment response. The emergence of resistance-associated mutations and the distinct immune profiles observed between responders and non-responders could inform future therapeutic strategies. Specifically, therapies targeting immune suppression or strategies to enhance immune activation could be beneficial for non-responders, while personalized treatments designed to target acquired resistance mutations in genes like *RAS*, *BRAF*, and *PIK3CA* could help overcome therapeutic barriers and improve outcomes in this challenging cohort.

#### 1. INTRODUCTION

#### 1.1. COLORECTAL CANCER (CRC)

#### 1.1.1. Epidemiology

Colorectal cancer (CRC) ranks in third place in terms of incidence and the second leading cause of cancer-related death worldwide (Figure 1), with more than with 1,9 million new cases and 904,000 deaths in 2022. High rates were in Europe (Eastern Europe), North America, Australia, New Zealand and Eastern Asia (Figure 2). According to the International Agency for Research on Cancer, men have about 44% higher risk of developing colorectal cancer in comparison to women<sup>1</sup> (Figure 3). Despite recent advances in colorectal cancer research have greatly enhanced overall survival rates in older adults, an increasing incidence is reported in high-income countries, as well as in young adults (<50 years) <sup>2</sup>.

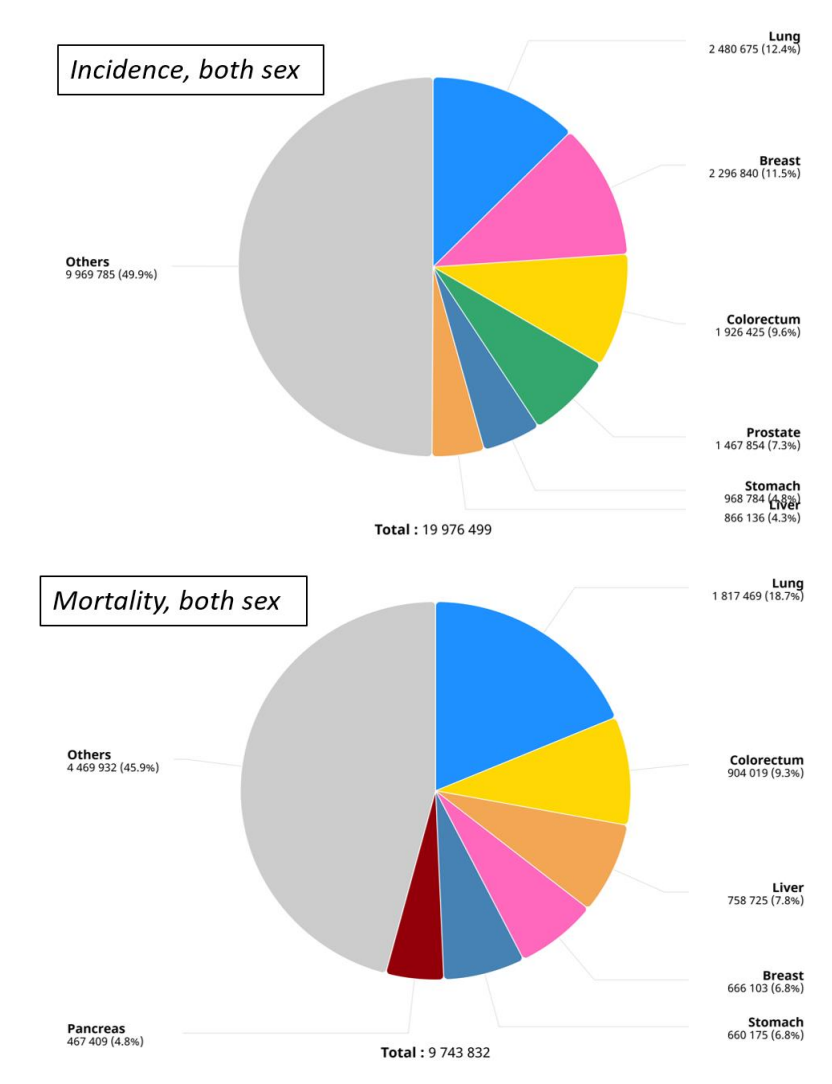


Figure 1. **Incidence and mortality of the most common cancers, in both sexes worldwide.** (Adapted from "The Global Cancer Observatory", November, 2024)

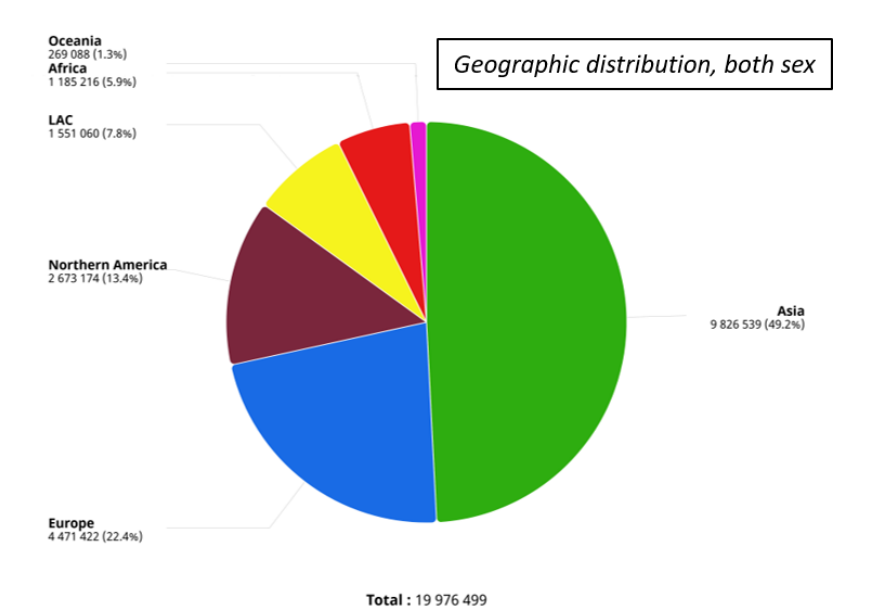


Figure 2. **Colorectal cancer incidence worldwide.** (Adapted from "The Global Cancer Observatory", November, 2024)

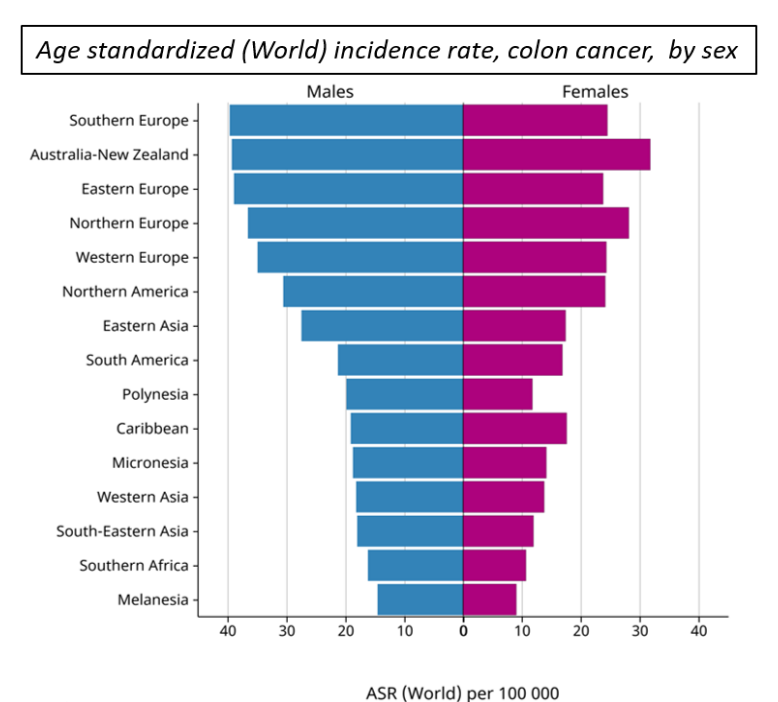


Figure 3. **Age standardized incidence rates\*** (**ASR**) **per 100.000 people.** \* ASR represents the annual number of new cases or deaths per 100,000 people that a population would experience if it had a typical age distribution. Standardization is necessary when comparing different populations with varying age structures, as age significantly impacts cancer risk.

#### 1.1.2. Etiology and risk factors

Colorectal cancer is a multifactorial disease, and its etiology is still not fully understood. Most often, CRC occurs as transformation within adenomatous polyps. About 80% of cases are sporadic, and 20% have an inheritable component<sup>2</sup>.

In regard to risk factors for CRC, encompassing both environmental and genetic influences, can be categorized into modifiable and non-modifiable factors<sup>3</sup>.

Modifiable risk factors for CRC are involved in the onset of sporadic CRC and include:

- Tobacco and alcohol use<sup>4–6</sup>;
- Metabolic dysregulation, such as obesity or metabolic syndrome<sup>2,7,8</sup>;
- Sedentary lifestyle<sup>9</sup>;
- Unhealthy diet (high consumption of red and processed meat) <sup>10</sup>.

#### Non-modifiable risk factors include:

- Age, in fact the risk of developing colorectal cancer increases with age, with the majority of cases occurring in individuals over 50<sup>2</sup>;
- Genetic predisposition: Several specific genetic conditions, most of which are inherited in an autosomal-dominant manner, are linked to a significantly increased risk of developing colon cancer. Familial adenomatous polyposis (FAP) and Lynch syndrome (hereditary nonpolyposis colorectal cancer [HNPCC]) are the most prevalent familial colon cancer syndromes. However, these two conditions together account for only about 5% of CRC cases, the majority of which are due to Lynch syndrome. Mutations in CRC predisponding-genes are the main cause of early-onset colorectal cancer (EOCRC, refers to adults <50 years old)<sup>3,11</sup>;
- Family history of CRC: Many studies have reported a higher risk of CRC in first-degree relatives of CRC patients, with relative risks (RRs) ranging from 2 to 4<sup>12</sup>;
- Personal history: certain comorbidities have been identified as risk factors for developing CRC. Individuals with inflammatory bowel disease (IBD), such as ulcerative colitis or Crohn's disease, are at an elevated risk for CRC<sup>13,14</sup>.

Although these factors cannot be controlled, they may be considered for identifying high-risk individuals or populations as candidates for preventive interventions<sup>2,3</sup>.

#### 1.1.3. Screening, surveillance and diagnosis of CRC

Most CRCs arise from precancerous lesions called adenomas, through the "adenoma-carcinoma sequence". This neoplastic transformation takes nearly 10 years and starts from polyps that progress from small to large, then to dysplasia and cancer. Both genetic factors, including mutations in driver genes, and environmental factors, such as exposure to risk factors, contribute to this process<sup>15,16</sup>. Screening for CRC enables to identify neoplastic lesions at an early stage and also precancerous lesions. It is evident that screening interventions have played a pivotal role in driving the rapid advancements observed in colorectal cancer (CRC) outcomes since the early 21st century. CRC screening has been demonstrated to not only mitigate the incidence of the disease but also significantly reduce mortality rates among individuals over the age of 50 with an average risk profile. A range of screening methodologies has been empirically validated for their efficacy in lowering both

CRC incidence and associated mortality, although the extent of this benefit is variable across different studies. Specifically, the observed reduction in incidence spans from 39% to 60%, while mortality reductions range from 55% to 80% when compared to non-screened populations<sup>17</sup>.

In recent years, many new screening methods have been studied, but the most commonly used ones remain the faecal immunochemical test (FIT) and colonscopy<sup>2</sup> (Figure 4).

FIT is the most widely applied home-based stool-based screening test due to its higher sensitivity. FIT test enables the detection of bleeding from the lower gastrointestinal tract associated with various types of lesions, including precancerous ones, without the need for dietary restrictions and with fewer stool samples required. This method is economic, noninvasive, well tolerated but it can yield false-positive results due to bleeding from other sources (e.g., hemorrhoids)<sup>15,18</sup>.

Colonscopy is a direct visualization method for assessing the entire colon through the insertion of a flexible tube with a camera (colonoscope) into the rectum. Colonscopy can also identify precancerous lesions, providing an opportunity for their removal. It can be used as an initial screening test or as a follow-up procedure after a positive result from another non-invasive test, such as FIT test. This technique is an invasive procedure that requires bowel preparation and carries a slight risk of complications, such as bleeding or perforation 15,19.

There are several other types of screening tests, less commonly used than those previously described:

- Stool-based tests, such as the Guaiac fecal occult blood test (gFOBT) and Multitarget stool DNA testing (sDNA-FIT);
- Direct visualization tests, such as virtual colonoscopy or sigmoidoscopy;
- Blood-based tests, which detect the molecular biomarker (methylated *SEPT9*) released into the bloodstream by colorectal cancer cells <sup>15,18,20</sup>.

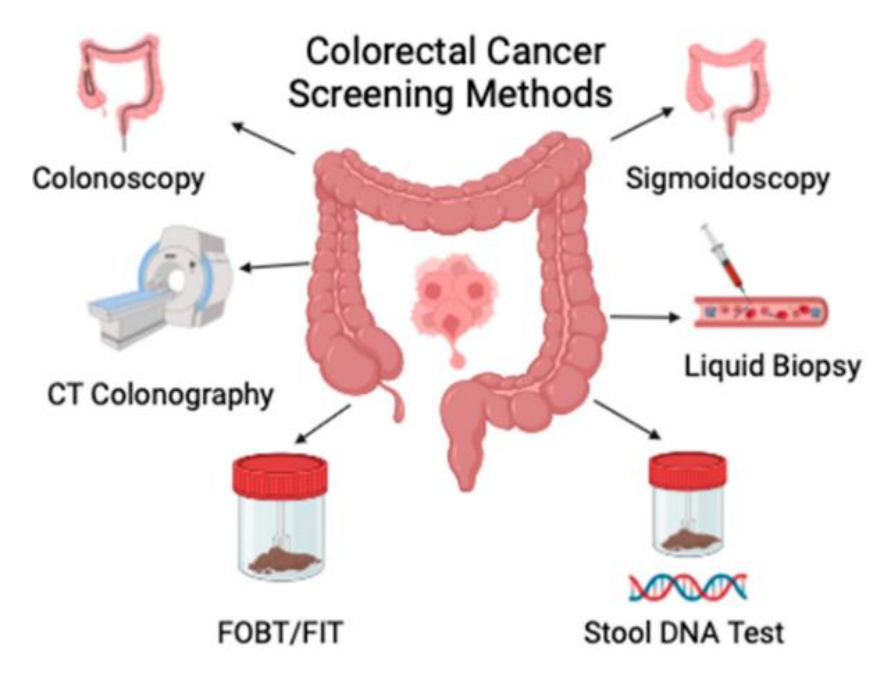


Figure 4. Overview of colorectal cancer screening methods. (Maida et. Al, Cancers, 2024)

There are several factors that improve risk of CRC in the general population. Risk stratification for initiating CRC screening or surveillance is essential to improve diagnosis and prognosis of CRC patients. Most CRCs are sporadic and risk increases with older age. These individuals are considered average-risk adults, in fact they have an approximate 4% lifetime risk of being diagnosed with CRC. In this populations screening is recommended starting at 45 years. If the test result is negative, strong evidence recommends retesting every year or every two years. However, if the result is positive, a colonoscopy should be used as a follow-up measure to confirm or rule out the presence of CRC.<sup>21</sup> Other factors that influence the recommendations for screening and surveilling CRC are:

- Family history: If a single first-degree relative has been diagnosed with CRC at the age of 60 years or older, screening with colonoscopy is recommended starting at age 40, to be repeated every 10 years. However, if a single first-degree relative was diagnosed with CRC before the age of 60, or if two or more first-degree relatives have had CRC or advanced adenomas at any age, screening with colonoscopy is recommended starting at age 40 or 10 years before the youngest family member's diagnosis, with colonoscopy repeated every 5 years<sup>22,23</sup>;
- Predisposing hereditary CRC syndromes: The most frequent syndromes are Familial Adenomatous Polyposis (FAP) and Hereditary Nonpolyposis Colorectal Cancer (HNPCC), also known as Lynch Syndrome. In FAP families, annual colonoscopy should begin at ages 20 to 25. While patients with attenuated FAP can be treated with polypectomy and regular monitoring, prophylactic colectomy is advised when the number of adenomas is too high or they are too challenging to remove through endoscopic polypectomy. Hence, for patients with

- HNPCC, annual colonoscopy may be suggested beginning at age 20–25, or 10 years before the age at which the first colon cancer diagnosis occurred in the family<sup>24,25</sup>;
- CRC predisposing conditions: patients with colonic inflammatory bowel disease (IBD) can be stratified as low-risk (colonoscopy every 3–4 years) or high-risk (colonoscopy every 1–2 years)<sup>26,27</sup>.

In regard to diagnosis of CRC, typical symptoms include hematochezia or melena, abdominal pain, unexplained iron deficiency anemia, changes in bowel habits, or a combination of these. Less frequently, patients may present with abdominal distension, nausea, vomiting, or a combination of these symptoms, which could suggest an obstruction<sup>28</sup>.

The main test used for colon cancer diagnosis remain colonoscopy. It allows to localize and biopsy lesions, detect synchronous neoplasm and extract polyps. Following a colon cancer diagnosis, additional tests may be required to determine how far the cancer has spread. The healthcare team takes the stage of the cancer into account when developing a treatment plan. Procedure for cancer staging include chest, abdomen and pelvic CT before surgical resection or initiation of treatment <sup>29</sup>.

#### 1.1.4. Molecular pathogenesis of CRC

Colorectal cancer (CRC) is a heterogeneous disease resulting from the accumulation of genetic and epigenetic alterations that disrupt the normal homeostasis of colonic epithelial cells, driving their progression to adenocarcinoma. The molecular pathogenesis of CRC is primarily governed by three key pathways, which underpin the biological diversity of CRC and its clinical behavior<sup>2,30–32</sup> (Figure 5):

- Chromosomal Instability (CIN): CIN is the most prevalent pathway, accounting for approximately 80% of CRC cases. It is characterized by large-scale genomic alterations, including aneuploidy, chromosomal translocations, and amplifications or deletions of entire chromosomal regions. CIN leads to the activation of oncogenes like *KRAS* and *MYC* while inactivating critical tumor suppressor genes such as *APC* and *TP53*. A hallmark of the CIN pathway is the early mutation of the *APC* gene, which disrupts the WNT signaling pathway, promoting unchecked cell proliferation. Subsequent mutations in *KRAS* drive further tumor growth, while *TP53* inactivation removes key cell-cycle checkpoints, facilitating tumor progression. CIN-driven tumors often exhibit glandular differentiation and are typically associated with left-sided CRC, progressing through the adenoma-carcinoma sequence.
- Microsatellite Instability (MSI): MSI accounts for approximately 15% of CRC cases and results from defective DNA mismatch repair (MMR) mechanisms. This defect is frequently caused by mutations in MMR genes such as *MLH1*, *MSH2*, *MSH6*, or *PMS2*, or by epigenetic

silencing of *MLH1* through promoter hypermethylation. MSI leads to a hypermutator phenotype, characterized by the accumulation of insertion-deletion mutations in repetitive DNA sequences, particularly microsatellites. Tumors with MSI are often hypermutated and exhibit unique molecular profiles, including frequent mutations in *BRAF* and immune-regulating genes. MSI tumors commonly arise in the proximal colon and are associated with increased immune infiltration, leading to better outcomes in early stages and a robust response to immune checkpoint inhibitors in advanced stages. MSI is also a hallmark of Lynch syndrome, a hereditary form of CRC, emphasizing its clinical significance in both sporadic and familial cases.

CpG Island Methylator Phenotype (CIMP): CIMP involves widespread hypermethylation of CpG islands in the promoter regions of tumor suppressor genes, leading to their silencing. This epigenetic alteration plays a critical role in CRC pathogenesis by inactivating genes involved in cell cycle regulation, DNA repair, and apoptosis, such as *MLH1*. CIMP-positive tumors are commonly associated with *BRAF V600E* mutations and are frequently observed in the proximal colon. These tumors often overlap with MSI cases due to the epigenetic silencing of *MLH1*, highlighting the interconnected nature of these pathways. CIMP-driven CRC represents a distinct subgroup with unique molecular and clinical features, offering opportunities for biomarker-driven diagnostics and therapies.

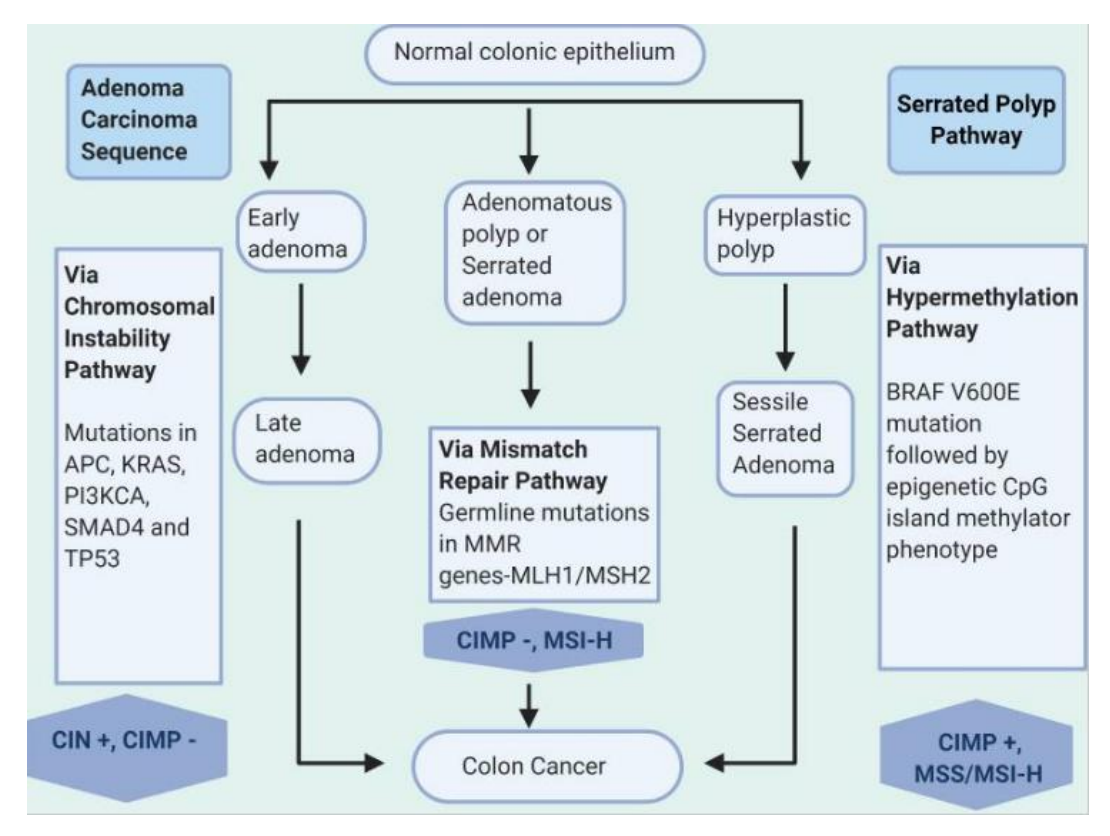


Figure 5. Molecular pathogenesis of CRC. Molecular pathways underlying the progression of colon cancer, illustrating

the adenoma-carcinoma sequence via chromosomal instability (CIN) and mismatch repair deficiency (MMR), alongside the serrated polyp pathway via hypermethylation. Key genetic and epigenetic alterations, including *APC*, *KRAS*, *BRAFV600E* mutations, and CpG island methylator phenotype (CIMP), are highlighted, showing the distinct yet convergent routes leading to malignancy (Kasi, Anup et al., 2020).

Beyond these primary pathways, other factors such as inflammation, microRNA dysregulation, and aberrant metabolic signaling further contribute to CRC pathogenesis. For example, microRNAs like miR-143 and miR-145 are often downregulated in CRC, affecting pathways like KRAS signaling. Additionally, global hypomethylation contributes to genomic instability, further fueling tumor development. These pathways collectively demonstrate the complexity and heterogeneity of CRC, underscoring the need for tailored diagnostic and therapeutic approaches. By understanding the interplay between CIN, MSI, and CIMP, as well as the broader molecular landscape, clinicians and researchers can refine strategies for early detection, prognostication, and precision medicine interventions in CRC<sup>2</sup>.

#### 1.1.5. Consensus Molecular Subtypes (CMSs) of CRC

The Consensus Molecular Subtypes (CMS) classification represents a pivotal advancement in understanding the heterogeneity of colorectal cancer (CRC). Established through comprehensive transcriptomic analyses, this framework categorizes CRC into four biologically and clinically distinct subgroups<sup>33,34</sup> (Table 1):

- CMS1 (MSI-Immune): Comprising approximately 14% of CRC cases, CMS1 is characterized by high microsatellite instability (MSI) and a hypermutated genome. Tumors in this subtype show robust immune activation, with dense lymphocytic infiltration, upregulation of immune checkpoint molecules (e.g., *PD-1*, *PD-L1*), and enhanced cytotoxic T-cell activity. These features make CMS1 tumors highly responsive to immune checkpoint inhibitors, particularly in advanced stages. Most CMS1 tumors arise in the proximal colon and are associated with *BRAF* mutations and hypermethylation of CpG islands (CIMP-high). While CMS1 tumors have a favorable prognosis in early stages due to immune surveillance, their prognosis worsens after metastasis or recurrence due to immune escape mechanisms;
- CMS2 (Canonical): The largest subgroup, accounting for about 37% of CRC cases, CMS2 is driven by chromosomal instability (CIN). These tumors exhibit epithelial differentiation and strong activation of the WNT and MYC signaling pathways, which promote cell proliferation and survival. CMS2 tumors are predominantly left-sided and demonstrate glandular histology, reflecting their epithelial nature. Clinically, CMS2 is associated with a good prognosis due to its relatively stable genome and responsiveness to conventional chemotherapeutic regimens.

However, these tumors are less responsive to immunotherapy, given their lower immune cell infiltration;

- CMS3 (Metabolic): CMS3 comprises around 13% of CRC cases and is defined by significant metabolic dysregulation. Tumors in this subtype show altered glucose and lipid metabolism, influenced by mutations in metabolic regulators such as *KRAS*. CMS3 tumors also exhibit epithelial characteristics but have lower immune cell infiltration compared to CMS1, contributing to their reduced immunogenicity. They are more commonly found in right-sided colon cancers. Despite their distinct metabolic profile, CMS3 tumors have an intermediate prognosis, partly because they lack strong responsiveness to both immunotherapy and conventional chemotherapy. Ongoing research is exploring the therapeutic potential of targeting metabolic vulnerabilities in this subtype;
- CMS4 (Mesenchymal): Representing approximately 23% of cases, CMS4 is associated with the worst prognosis among all subtypes. These tumors are characterized by epithelial-tomesenchymal transition (EMT), extensive stromal invasion, and activation of TGF-β signaling pathways. CMS4 tumors also exhibit increased angiogenesis immunosuppressive microenvironments, contributing to their aggressive behavior and resistance to standard therapies. This subtype is enriched with stromal and inflammatory cells, reflecting its mesenchymal phenotype. CMS4 tumors frequently present with advanced disease, higher rates of metastasis, and poor relapse-free and overall survival. Research into stromal-targeting therapies and EMT inhibitors is ongoing to improve outcomes for this challenging subtype.

	CMS1 (MSI Immune)	CMS2 (Canonical)	CMS3 (Metabolic)	CMS4 (Mesenchymal)
Proportion	14%	37%	13%	23%
Genetic Features	MSI, CIMP high, hypermutation	CIN high, SCNA high	Mixed MSI status, SCNA low, CIMP low	CIN high, SCNA high
Mutations	BRAF mutations		KRAS mutations	
Molecular Pathways	JAK-STAT	WNT and MYC activation	Metabolic deregulation	EMT, TGF-β activation, angiogenesis
ТМЕ	Immune infiltration and activation	Immune desert	Immune desert	Stromal infiltration, fibroblastic infiltration, immunosuppression
Prognosis (Stage I-III)	Good	Good	Good	Poor
Prognosis (Stage IV)	Poor	Good	Intermediate	Intermediate

Table 1. Comprehensive classification of colorectal cancer molecular subtypes (CMS) based on key genetic, epigenetic, and tumor microenvironment (TME) characteristics. Prognostic implications for stages I-III and IV are outlined for CMS1 (MSI Immune), CMS2 (Canonical), CMS3 (Metabolic), and CMS4 (Mesenchymal) subtypes, highlighting variations in mutation profiles, molecular pathways, and immune landscape. Acronyms used: MSI – Microsatellite Instability, CIMP – CpG Island Methylator Phenotype, CIN – Chromosomal Instability, SCNA – Somatic Copy Number Alteration, TME – Tumor Microenvironment, EMT – Epithelial-Mesenchymal Transition, TGF- $\beta$  – Transforming Growth Factor Beta. (Adapted from Guinney, J., et al. Nat Med 21, (2015) and Sophie Mouillet-Richard, et al. Clin Cancer Res, June 2024)

The CMS framework not only highlights the biological diversity of CRC but also correlates strongly with patient outcomes and therapeutic responses. CMS1 and CMS2 tumors generally exhibit favorable prognoses in early stages, while CMS3 and CMS4 subtypes face greater therapeutic challenges due to intrinsic resistance mechanisms. This stratification underscores the need for precision medicine in CRC, offering a pathway to subtype-specific treatments that address the unique molecular and clinical characteristics of each CMS group.

#### 1.1.6. Staging of CRC

The staging of colorectal cancer (CRC) plays a pivotal role in clinical practice, guiding treatment decisions, predicting prognosis, and informing the management of the disease. Accurate staging is essential for tailoring therapeutic interventions and evaluating the potential for curative surgery, adjuvant chemotherapy, or palliative care. The most widely adopted system for staging is the TNM classification, developed by the American Joint Committee on Cancer (AJCC) and the Union for International Cancer Control (UICC). This system evaluates three essential parameters: T (tumor), N (lymph nodes), and M (metastasis)<sup>35</sup>.

The "T" category describes the extent of primary tumor invasion into the colonic or rectal wall and adjacent structures. It is categorized from T0 to T4, with higher numbers indicating deeper and more extensive invasion:

- T1, represents invasion into the submucosa;
- T2 denotes invasion into the muscularis propria;
- T3 signifies invasion through the muscularis propria into the serosa or nearby structures;
- T4 indicates tumor invasion into adjacent organs or the peritoneum.

The "N" classification refers to the presence and extent of regional lymph nodes involvement. Lymph node interest is a critical factor in determining prognosis, as it is associated with an increased risk of systemic spread and recurrence. It is classified as:

• N0, indicating no nodal involvement;

- N1, metastasis to 1-3 regional lymph nodes;
- N2, metastasis to 4 or more regional lymph nodes;

The "M" classification addresses the presence of distant metastasis, with:

- M0, signifying no distant spread;
- M1, indicating metastatic disease, typically to the liver, lungs, peritoneum or other distant organs.

After determining an individual's T, N, and M categories, this data is integrated through a process known as stage grouping to assign the overall cancer stage between 1 and 4<sup>36,37</sup>:

- Stage I (Localized Disease, T1–T2, N0, M0): Tumors are confined to the colonic or rectal wall. The 5-year survival rate for Stage I CRC can exceed 90%, highlighting the importance of early detection and surgical treatment for optimal outcomes;
- Stage II (Locally Advanced Disease, T3–T4, N0, M0): This stage is marked by tumor invasion through the muscularis propria (T3) or into surrounding organs (T4), but without lymph node involvement or distant spread. These tumors have a higher likelihood of local recurrence due to their deeper penetration. The 5-year survival rate for Stage II CRC ranges from 70% to 90%, depending on the presence of additional risk factors;
- Stage III (Regional Lymph Node Metastasis, any T, N1–N2, M0): At this stage, tumors have spread to nearby lymph nodes but have not yet metastasized to distant organs. Treatment requires a combination of surgery and adjuvant chemotherapy to reduce the risk of recurrence. The presence of regional lymph node metastasis increases the chance of recurrence and potential systemic spread. The 5-year survival rate for Stage III CRC varies from 40% to 70%, depending on the extent of lymph node involvement and other risk factors;
- Stage IV (Metastatic Disease, any T, any N, M1): In Stage IV CRC, distant metastasis (M1) is present, often affecting the liver, lungs, peritoneum, or other organs. Prognosis is generally poor, with a 5-year survival rate of less than 15%.

The TNM system remains the gold standard for staging, but the advent of molecular and genetic profiling has further refined the staging process, enabling personalized treatment strategies. Genetic mutations in KRAS, NRAS, and BRAF genes, along with microsatellite instability (MSI) status, provide critical prognostic information and may influence treatment decisions. In fact, patients with MSI-high tumors are more likely to respond to immune checkpoint inhibitors, whereas those with *KRAS* mutations may not benefit from anti-*EGFR* therapies<sup>33,38,39</sup>.

In conclusion, colorectal cancer staging is a complex, multi-faceted process that combines clinical, pathological, and molecular factors to determine the extent of disease, guide therapeutic interventions, and predict patient outcomes<sup>40</sup>.

#### 1.1.7. Treatment and follow-up of CRC

CRC treatment strategies are highly personalized, considering the stage of the disease, the patient's overall health, and advancements in molecular profiling. According to established clinical guidelines, treatment protocols differ substantially across disease stages. While early-stage CRC often necessitates surgical intervention alone, advanced stages demand a multidisciplinary approach that incorporates systemic therapies, targeted treatments, and, where possible, curative or palliative local interventions to optimize outcomes.

For Stage 0 CRC, treatment is relatively straightforward. Lesions confined to the mucosal layer are frequently removed via polypectomy during a colonoscopy. For larger lesions or cases with suspected invasive potential, more extensive surgical resection may be required to ensure complete removal. Post-treatment surveillance is critical, with follow-up colonoscopy recommended within 3–6 months to confirm healing and detect any additional lesions<sup>41</sup>.

In Stage I CRC, surgical resection is the mainstay of treatment. Procedures such as colectomy with lymphadenectomy (removal of at least 12 regional lymph nodes for accurate staging) are standard. Chemotherapy is generally not required due to the excellent prognosis, with most patients achieving high survival rates following surgery alone. Long-term monitoring, including colonoscopy 1–2 years after surgery and then every 3–5 years, ensures early detection of recurrence or new lesions<sup>41</sup> (Figure 6).

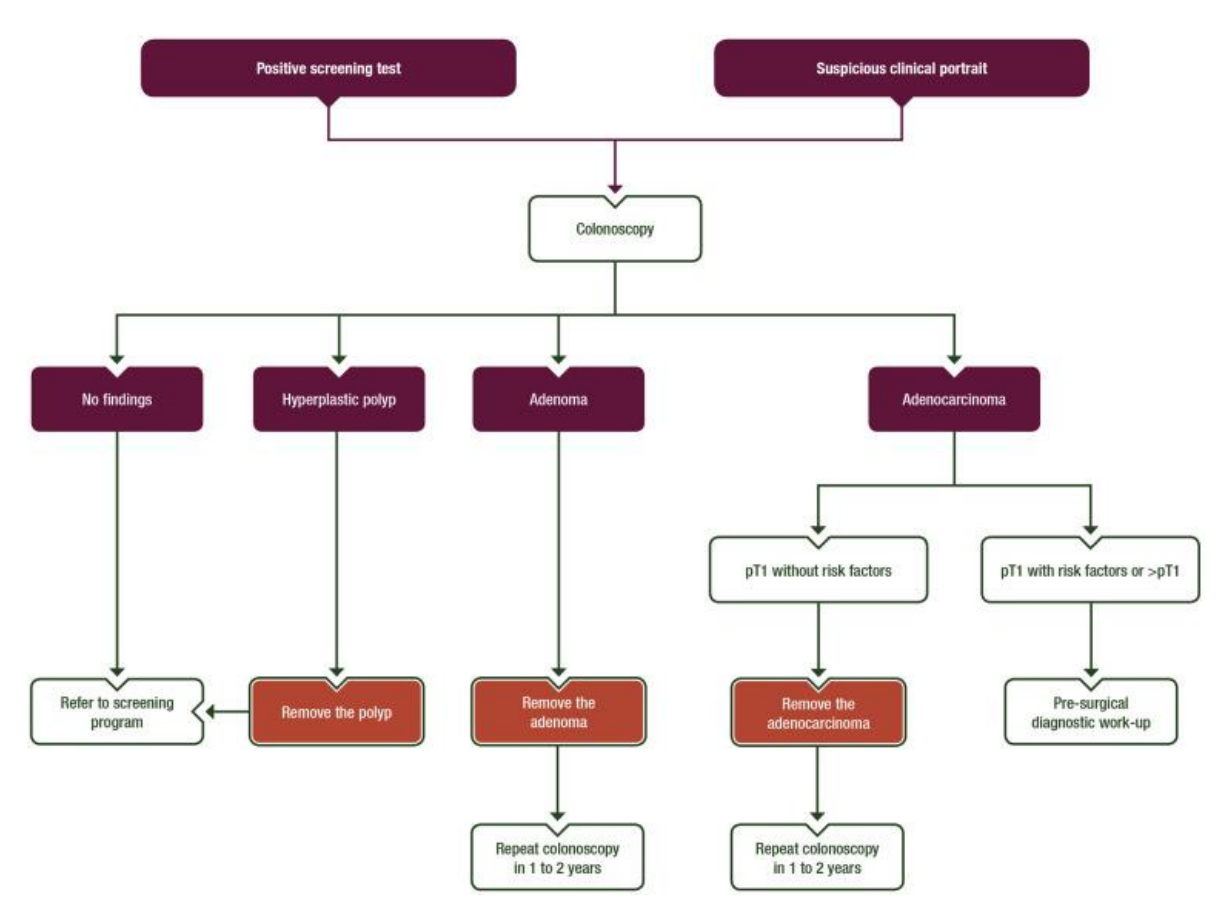


Figure 6. **Diagnostic and treatment pathway for stage 0 and I colorectal cancer (CRC).** Following a positive screening test or a suspicious clinical presentation, colonoscopy is performed. Outcomes include no findings (referral back to screening), hyperplastic polyp removal, adenoma removal with follow-up colonoscopy in 1-2 years, or adenocarcinoma management based on the presence of risk factors, ranging from localized removal to pre-surgical diagnostic work-up for advanced cases. (Argilés G, et al. Ann Oncol. 2020)

Treatment for Stage II CRC focuses on surgical resection with curative intent. In low-risk cases, surgery alone (e.g., colectomy with lymphadenectomy) is sufficient. However, for high-risk patients—those with factors such as T4 tumors, lymphovascular or perineural invasion, perforation, or bowel obstruction—adjuvant chemotherapy may be warranted. Commonly used regimens include fluoropyrimidine-based therapies like capecitabine or 5-fluorouracil (5-FU), which reduce the likelihood of recurrence. Molecular testing for microsatellite instability (MSI) or mismatch repair deficiency (dMMR) is vital, as tumors with MSI-H/dMMR tend to have a better prognosis and may not benefit from chemotherapy. Follow-up includes regular imaging (CT or MRI) and colonoscopies<sup>41</sup> (Figure 7).

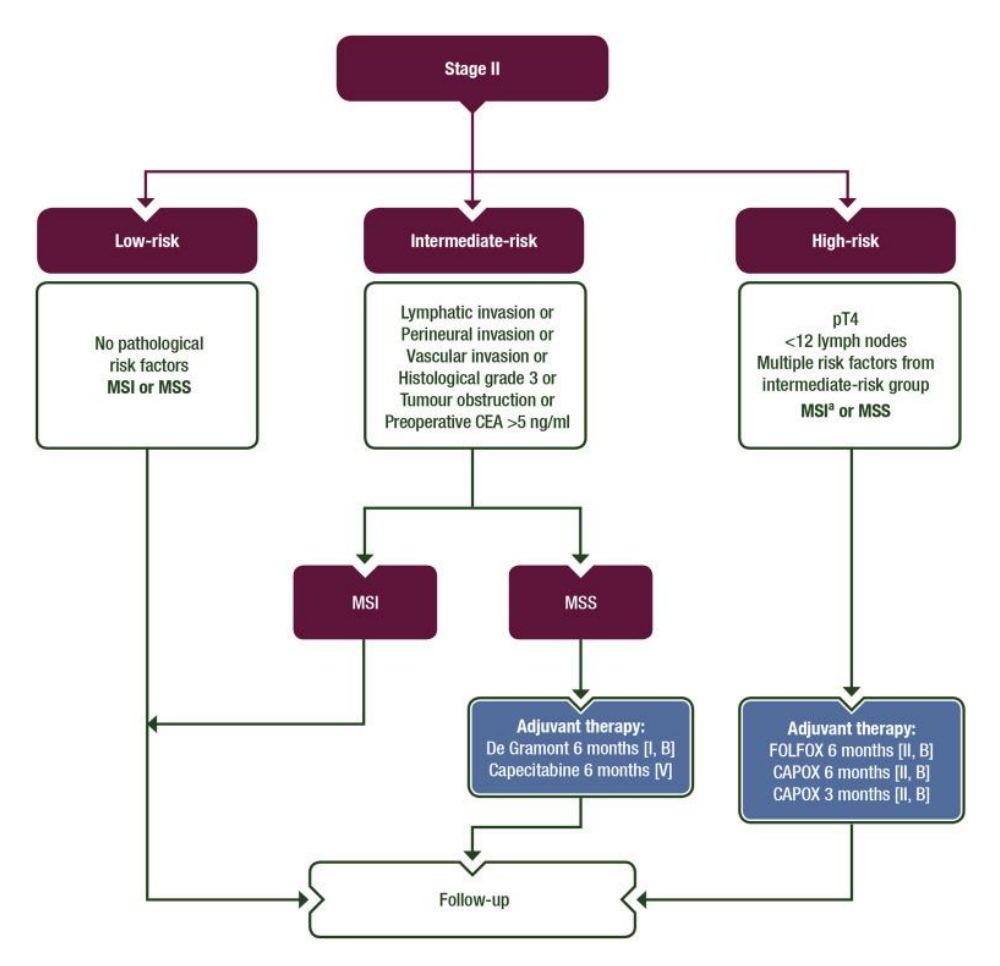


Figure 7. Management pathway for stage II colorectal cancer (CRC) based on risk stratification. Patients are categorized as low-risk, intermediate-risk, or high-risk based on pathological and clinical features. Low-risk patients typically undergo follow-up, while intermediate- and high-risk patients may require adjuvant therapy tailored to microsatellite instability (MSI) or microsatellite stability (MSS) status, including regimens such as De Gramont, Capecitabine, FOLFOX, or CAPOX. (Argilés G, et al. Ann Oncol. 2020)

In Stage III CRC, where regional lymph node involvement is present, treatment becomes more aggressive. Surgery remains the initial step, involving tumor resection and lymphadenectomy. Adjuvant chemotherapy is essential to target micrometastatic disease and minimize the risk of recurrence. Standard regimens include FOLFOX (5-FU, leucovorin, oxaliplatin) or CAPOX (capecitabine, oxaliplatin), with treatment durations ranging from 3 to 6 months depending on the patient's overall health and risk factors. For patients unable to tolerate oxaliplatin, fluoropyrimidine monotherapy is an alternative. Long-term follow-up involves imaging and CEA monitoring every 3–6 months for the first 2 years and annually thereafter for up to 5 years<sup>41</sup> (Figure 8).

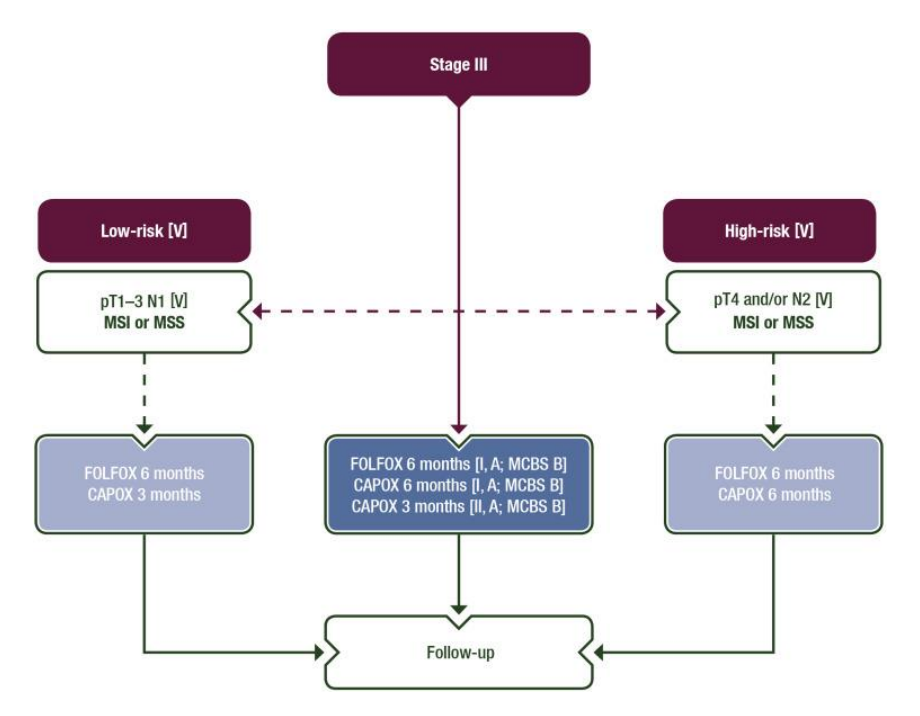


Figure 8. Management approach for stage III colorectal cancer (CRC) stratified by risk level. Low-risk (pT1–3 N1) and high-risk (pT4 and/or N2) patients, determined by MSI or MSS status, are treated with adjuvant chemotherapy using FOLFOX or CAPOX regimens for either 3 or 6 months, based on the level of risk. Follow-up care is provided after completion of treatment. (Argilés G, et al. Ann Oncol. 2020)

In regard to advanced stage (IV), mCRC presents one of the most complex challenges in oncology. Treatment is primarily focused on prolonging survival, alleviating symptoms, and, in select cases, achieving remission or cure. The management strategy depends on the extent of metastatic disease and patient suitability for specific therapies.

For patients with limited metastases, such as those confined to the liver or lungs, surgery offers a chance for long-term remission or cure. Complete resection of all visible disease can result in five-year survival rates as high as 45%. Perioperative chemotherapy is often employed to improve outcomes. Even patients with initially unresectable metastases may become candidates for surgery following systemic therapy that successfully shrinks the tumors<sup>42</sup>.

For isolated metastatic lesions, localized treatments can serve as alternatives or adjuncts to surgery (Figure 9):

- Ablation Therapies: Techniques like radiofrequency ablation (RFA) or microwave ablation (MWA) effectively destroy small tumors, particularly in the liver or lungs, and are especially useful for patients ineligible for surgery.
- Stereotactic Body Radiotherapy (SBRT): This high-precision, high-dose radiation therapy minimizes damage to surrounding tissues and achieves excellent local control.

HIPEC (Hyperthermic Intraperitoneal Chemotherapy): For metastases in the peritoneum, this
specialized therapy delivers heated chemotherapy directly into the abdominal cavity postsurgery.

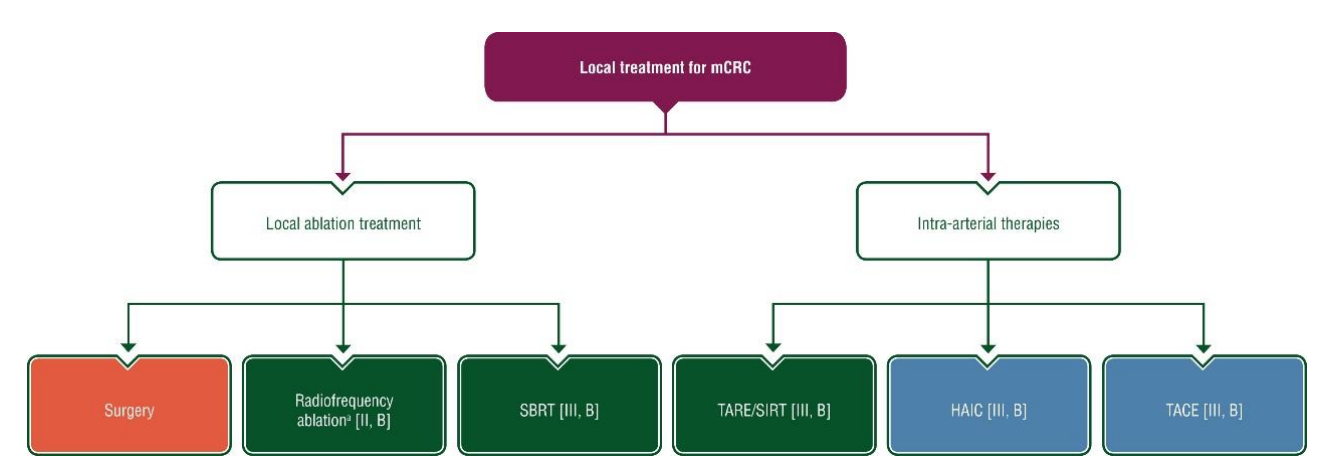


Figure 9. Overview of local treatment options for metastatic colorectal cancer (mCRC), including local ablation treatments such as surgery, radiofrequency ablation, and stereotactic body radiotherapy (SBRT), as well as intra-arterial therapies such as transarterial radioembolization/selective internal radiation therapy (TARE/SIRT), hepatic arterial infusion chemotherapy (HAIC), and transarterial chemoembolization (TACE). (Cervantes A, et al. Ann Oncol. 2023)

For patients whose metastases are widespread and not surgically removable or the patient isn't well enough to handle an operation. For these patients, systemic therapy remains the primary treatment, and the goal shifts to controlling the disease and maintaining quality of life. Targeted treatments, palliative care, and even experimental therapies in clinical trials may all play a role. Local therapies like RFA or SBRT can still be used to manage symptoms or slow the progression of isolated lesions. Systemic therapy remains the cornerstone of treatment for metastatic CRC and is the standard approach for managing widespread or unresectable metastatic disease. Here, personalization is key, with treatment tailored based on the molecular profile of the tumor<sup>42</sup> (Figure 10):

- First-Line Chemotherapy: Patients typically start with combinations like FOLFOX (5-FU, leucovorin, oxaliplatin) or FOLFIRI (5-FU, leucovorin, irinotecan). These are often paired with targeted therapies to boost their effectiveness. For example, bevacizumab (which inhibits blood vessel growth) is commonly added, while cetuximab or panitumumab (which block the EGFR pathway) are options for patients with RAS wild-type tumors. The location of the primary tumor (left-sided or right-sided) also influences the choice of targeted therapies;
- Molecularly Tailored Treatments: Tumor biology really matters in metastatic CRC. If the tumor has high microsatellite instability (MSI-H) or deficient mismatch repair (dMMR), immune checkpoint inhibitors like pembrolizumab are a game-changer, often working where chemotherapy might not. For *BRAF*-mutant tumors, combinations like encorafenib (a BRAF)

inhibitor) with cetuximab are used in second/third-line therapy. And for *HER2*-positive tumors, anti-*HER2* therapies offer new options. These therapies target the unique "fingerprints" of the tumor, making treatments more effective and sparing unnecessary side effects.

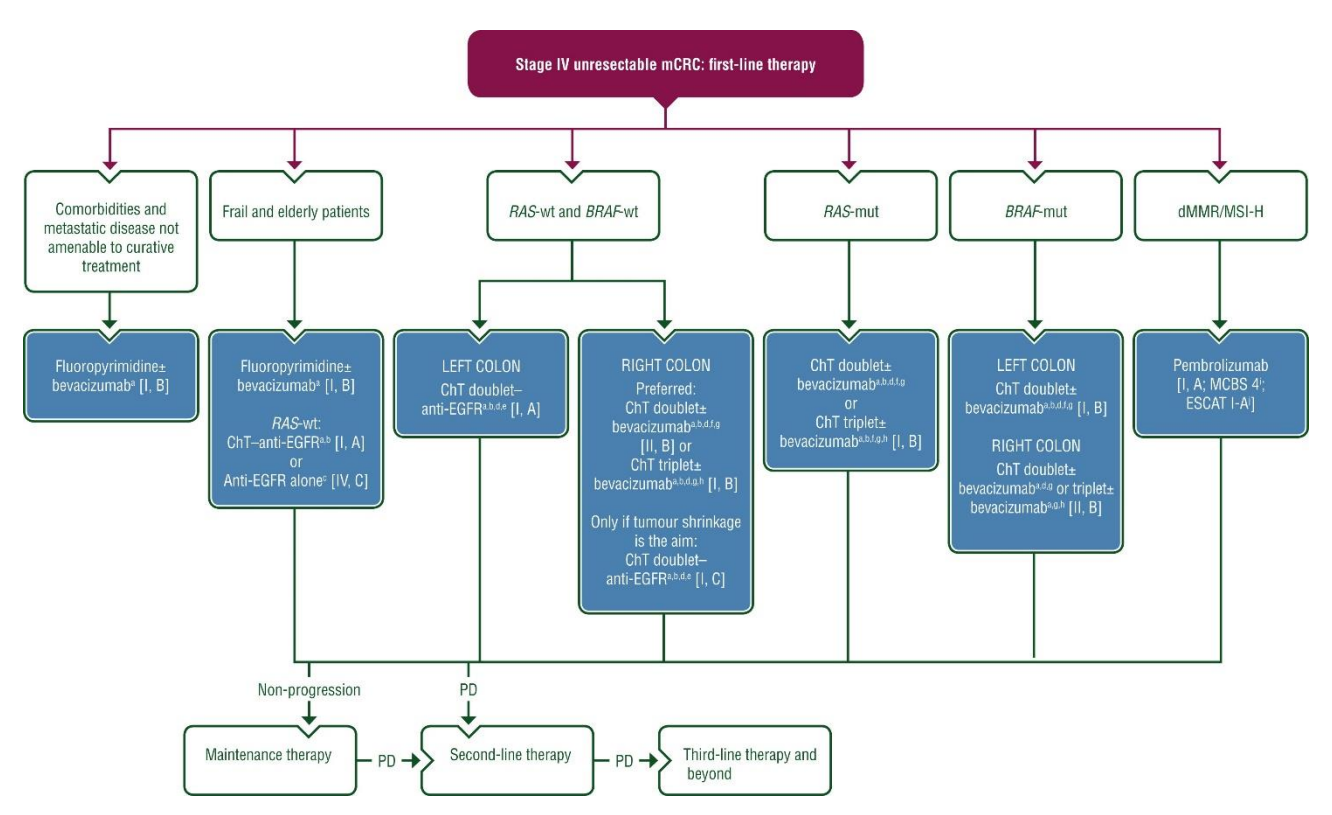


Figure 10. Treatment algorithm for stage IV unresectable metastatic colorectal cancer (mCRC) as first-line therapy. Management strategies are based on patient factors (e.g., comorbidities, frailty) and tumor molecular characteristics (e.g., RAS/BRAF mutation status, dMMR/MSI-H status). Therapy options include fluoropyrimidine-based regimens, anti-EGFR agents, chemotherapy doublets or triplets with/without bevacizumab, and pembrolizumab for dMMR/MSI-H tumors. Subsequent steps involve maintenance therapy, second-line, and third-line treatments upon progression. (Cervantes A, et al. Ann Oncol. 2023)

Regular monitoring is a huge part of managing metastatic CRC. Imaging studies (like CT or MRI scans) and blood tests for markers like CEA (carcinoembryonic antigen) help track how well treatments are working and detect any recurrence or progression<sup>42</sup>.

#### 1.1.8. Liquid Biopsy in CRC

Liquid biopsy is a cutting-edge diagnostic and prognostic tool that has revolutionized cancer management by enabling the non-invasive detection and analysis of tumor-derived components from biological fluids such as blood, urine, or cerebrospinal fluid. Unlike traditional tissue biopsy, which is invasive and provides only a single snapshot of tumor biology, liquid biopsy offers a dynamic, real-

time window into the molecular landscape of cancer. The technique encompasses the analysis of circulating tumor cells (CTCs), circulating tumor DNA (ctDNA), tumor-derived extracellular vesicles like exosomes, and tumor-associated platelets (TEPs), making it a versatile and comprehensive approach to cancer diagnostics. Its non-invasive nature, capacity for repeat sampling, and ability to capture tumor heterogeneity and monitor disease progression in real time make it an invaluable tool in the era of precision oncology<sup>43</sup>.

In CRC, liquid biopsy is emerging as a transformative modality for diagnosis, prognosis, and therapeutic monitoring. Traditional detection methods such as colonoscopy, tissue biopsy, and imaging, while effective, are invasive, time-consuming, and often unsuitable for frequent monitoring. Liquid biopsy addresses these limitations by providing a more accessible and patient-friendly approach to tumor surveillance<sup>44</sup> (Figure 11).

ctDNA, fragmented DNA released into the bloodstream by apoptotic or necrotic tumor cells, has demonstrated extraordinary potential as a biomarker in CRC. ctDNA contains the same genetic and epigenetic alterations as the primary tumor, including mutations, copy number variations, and methylation patterns, enabling a precise reflection of the tumor's molecular characteristics. Advanced detection methods such as high-resolution PCR, next-generation sequencing (NGS), and methylation-specific PCR have improved ctDNA sensitivity and specificity, allowing its application in various clinical contexts<sup>45,46</sup>:

- Early Detection and Screening: ctDNA is highly valuable in early CRC detection, with studies showing elevated levels of tumor-specific mutations in ctDNA from patients compared to healthy controls. For example, panels targeting frequently mutated genes in CRC, combined with protein biomarkers, have been shown to achieve high specificity and acceptable sensitivity for detecting early-stage cancers;
- Post-Surgical Monitoring and Minimal Residual Disease (MRD): After curative surgery, ctDNA can identify the presence of MRD, which often precedes clinical or radiological signs of recurrence. For instance, studies have shown that persistent ctDNA post-surgery correlates strongly with disease relapse, even in the absence of radiologically detectable disease. This ability to stratify patients based on residual tumor burden allows for tailoring adjuvant therapies more effectively, potentially sparing patients unnecessary toxicity from chemotherapy;
- Monitoring Treatment Response and Resistance: ctDNA levels dynamically reflect treatment response, enabling real-time assessment of therapeutic efficacy. Moreover, ctDNA can capture the emergence of resistance mutations, such as *RAS* mutations during anti-EGFR therapy in metastatic CRC (mCRC), guiding clinicians to switch to alternative treatments.

This real-time tracking offers a critical advantage over tissue biopsies, which are static and may not represent the evolving tumor biology.

In contrast, circulating tumor cells (CTCs) and tumor-derived vesicles like exosomes, while less broadly applied, still hold significant promise in CRC management. CTCs, rare cells shed from the primary tumor into the bloodstream, are valuable for understanding metastatic potential and disease progression. Advanced enrichment and detection technologies, such as immunomagnetic separation and size-based filtration, have improved their detection rates. Elevated CTC counts are often associated with worse prognosis, and their molecular characterization, including epithelial-mesenchymal transition (EMT) markers, provides insights into metastasis and therapy resistance. Exosomes, nano-vesicles secreted by tumor cells, carry diverse biomolecules such as proteins, miRNAs, and long non-coding RNAs, reflecting the tumor's physiological state. These vesicles show promise as biomarkers for disease monitoring and therapeutic resistance, with exosomal miRNAs like miR-21 and miR-1246 being linked to CRC progression and metastasis.

Despite its transformative potential, several challenges remain for liquid biopsy to achieve widespread clinical adoption. Standardization of pre-analytical and analytical methods, particularly for ctDNA and CTC detection, is critical to ensure reproducibility across laboratories. Sensitivity for detecting early-stage CRC and low-abundance biomarkers must be improved to expand its utility in population screening. Moreover, the integration of liquid biopsy into clinical workflows will require regulatory approval and the establishment of robust clinical validation studies. Nonetheless, ongoing clinical trials and technological advancements continue to address these hurdles. The integration of liquid biopsy with machine learning algorithms and multi-omics approaches promises to enhance the sensitivity and specificity of CRC diagnostics further. As research progresses, liquid biopsy is poised to become an indispensable tool in the precision medicine framework for CRC, enabling earlier detection, personalized treatment strategies, and improved patient outcomes while minimizing the burden of invasive procedures 47,48.

#### Liquid biopsy Advantages C. Early Screening B. Repeatability for samples A. Non-invasive E. Overcoming tumor heterogeneity F. Predicting recurrence and D. To assist the tumor staging in the treatment process metastasis of the disease Application A Early Diagnosis CTCs Positive Examination of colonoscopy cfDNA/ctDNA The choice of treatment strategy PCR Surgery Chemotherapy Radiation TEPS therapy Assessment of disease prognosis Dynamic monitoring and Recurrence Predict recurrence

Figure 11. **The benefits and applications of liquid biopsy in CRC.** Liquid biopsy offers significant benefits, including its non-invasive nature, ability to allow repeatable sampling, effectiveness in early screening, assistance in tumor staging, and prediction of CRC recurrence and metastasis. Its applications include early CRC diagnosis, selection of treatment strategies, monitoring treatment responses, and evaluation of patient prognosis (Tao, XY., et al. Mol Cancer, 2024).

## 1.2. BRAFV600E-MUTATED METASTATIC COLORECTAL CANCER (BRAF<sup>V600Emut</sup> mCRC)

#### 1.2.1. BRAF gene: Mechanisms, Mutations, and Implications in CRCs

The *BRAF* gene encodes a serine/threonine-protein kinase that is a key component of the mitogen-activated protein kinase (MAPK) signaling pathway, which regulates vital cellular processes, including proliferation, differentiation, survival, and apoptosis. This pathway is activated when receptor tyrosine kinases (RTKs) such as epidermal growth factor receptor (EGFR) bind to their respective ligands, leading to the recruitment of adaptor proteins and the activation of RAS, a GTPase that acts as a molecular switch. Active RAS recruits BRAF to the cell membrane, where BRAF is phosphorylated and forms active dimers. These dimers phosphorylate and activate mitogen-activated protein kinase kinases (MEK1/2), which subsequently activate extracellular signal-regulated kinases (ERK1/2). Activated ERK translocates to the nucleus to regulate the transcription of genes that drive cell cycle progression, proliferation, and survival<sup>49,50</sup> (Figure 12).

In colorectal cancer, aberrations in the MAPK pathway are frequently driven by mutations in the *BRAF* gene, with *BRAFV600E* being the most common alteration. This mutation results in a valine-to-glutamic acid substitution at codon 600, leading to constitutive activation of BRAF independent of upstream RAS signals. This causes persistent activation of MEK and ERK, resulting in unchecked cell proliferation and survival, even in the absence of external growth signals. Such dysregulation contributes significantly to tumorigenesis and is associated with the aggressive biological behavior of *BRAFV600E*-mutant CRC<sup>51</sup>.

BRAF mutations in CRC can be categorized into three functional classes, each with distinct roles in the MAPK pathway. Class I mutations, such as BRAFV600E, act as highly active monomers that are RAS-independent and drive robust downstream signaling. Class II mutations, such as K601E or G469R, function as constitutive dimers and are also independent of RAS but exhibit intermediate kinase activity compared to class I. Class III mutations, including D594G and G466E, exhibit reduced intrinsic kinase activity and rely entirely on upstream RAS activation for their oncogenic effects. These mutations amplify upstream signals through heterodimerization with CRAF or wild-type BRAF. The functional diversity of these mutation classes underpins the complexity of MAPK pathway dysregulation in CRC<sup>52,53</sup>.

In addition to its oncogenic mutations, BRAF's role in cellular homeostasis is tightly regulated under normal physiological conditions by feedback mechanisms. In cancer, however, these feedback loops are often disrupted, allowing sustained MAPK signaling and promoting tumor progression. The unique biological features of *BRAF*-mutant CRC, such as its association with the serrated neoplasia pathway and CpG island methylator phenotype (CIMP), highlight the distinct molecular and clinical landscape of this tumor subtype<sup>51,54</sup>.

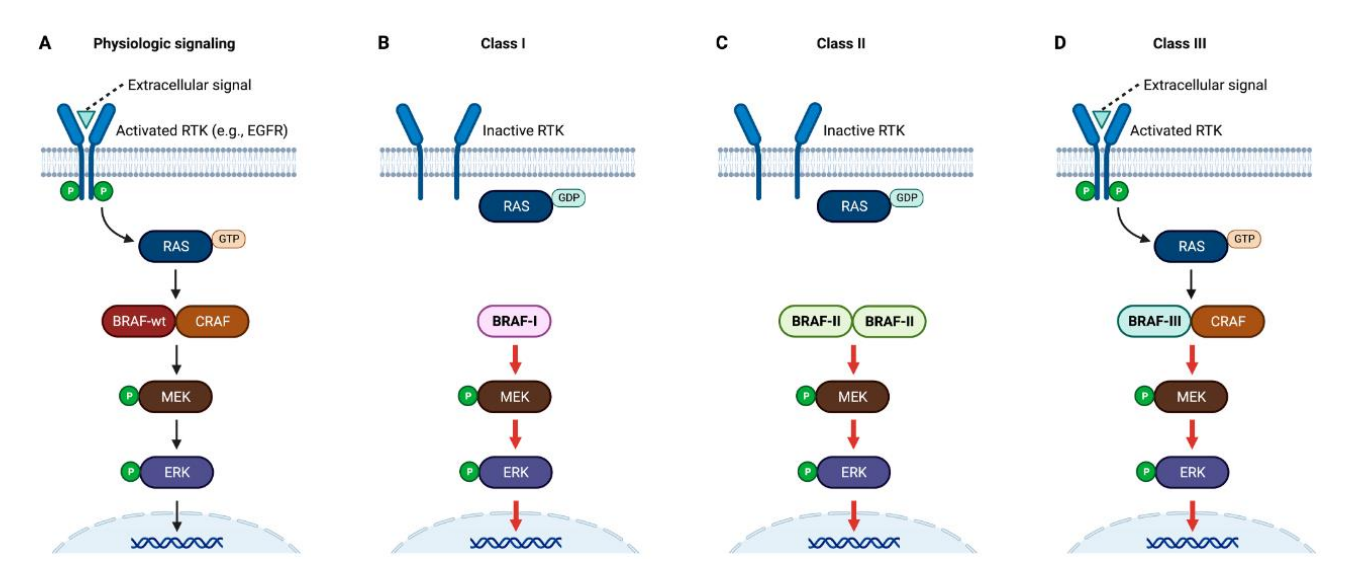


Figure 12. Schemes of the RAS-RAF-MEK-ERK pathway. In normal conditions, external signals activate receptor

tyrosine kinases (RTKs), leading to RAS activation and RAF dimerization (e.g., BRAF-CRAF), which sequentially phosphorylates MEK and ERK (A). Class I *BRAF* mutations (e.g., V600) activate downstream signaling independently of upstream input (B). Class II mutations are non-V600, dimer-dependent, and hyperactive (C). Class III mutations impair BRAF's kinase function but enhance downstream signaling through RAS activation (D). Each class exhibits unique characteristics, though variations exist within these categories. (Image from: Liu, J.; Xie, H., 2023)

#### 1.2.2. Clinical-pathological and molecular features of $BRAF^{V600Emut}$ mCRC

*BRAF*<sup>V600Emut</sup> CRC accounts for approximately 8-12% of metastatic cases. It is a distinct molecular and clinical subset characterized by unique pathological features, aggressive behavior, and poor response to conventional therapies<sup>55</sup>.

*BRAF*<sup>V600Emut</sup> CRC typically arises in the proximal colon and is strongly associated with the serrated neoplasia pathway. This pathway involves the progression of serrated polyps, particularly sessile serrated adenomas (SSAs), which frequently harbor the *BRAFV600E* mutation. These lesions demonstrate a transition from benign to malignant states through a series of molecular alterations, including widespread DNA methylation and silencing of tumor suppressor genes. The mutation drives constitutive activation of the mitogen-activated protein kinase (MAPK) signaling cascade, resulting in uncontrolled cellular proliferation and survival<sup>49,56,57</sup>.

Histologically, *BRAF*<sup>V600Emut</sup> CRCs are often poorly differentiated and exhibit features such as mucinous histology and serrated glandular architecture. Mucinous adenocarcinomas (reported in up to 19% of cases), characterized by abundant extracellular mucin, are a hallmark of these tumors and are associated with a more aggressive clinical course. Additional features include tumor budding, an infiltrative growth pattern, lymphovascular invasion and the presence of signet ring cells in some cases, further underscoring their aggressive nature<sup>53,58</sup>.

At the molecular level, BRAFV600E-mutated CRC is defined by constitutive activation of the MAPK pathway, driven by the substitution of valine with glutamic acid at codon 600 in the BRAF protein. These tumors are frequently associated with CIMP, characterized by widespread promoter hypermethylation, including silencing of *MLH1*. Approximately 20–40% of *BRAFV600E*-mutated CRC cases exhibit MSI due to *MLH1* hypermethylation. MSI-high (MSI-H) tumors are characterized by high mutational burdens and an immunogenic tumor microenvironment, which contributes to better responses to immune checkpoint inhibitors (ICIs). In contrast, the majority of *BRAF*<sup>V600Emut</sup> mCRC are microsatellite stable (MSS). These tumors are less immunogenic and demonstrate aggressive clinical behavior, frequently acquiring additional genetic alterations such as *TP53* and *PIK3CA* mutations, which exacerbate their malignant potential<sup>49,58,59</sup>.

Recent transcriptomic analyses have further stratified  $BRAF^{V600Emut}$  mCRC into subtypes, such as BM1 and BM2, based on gene expression profiles<sup>59,60</sup>:

- BM1 subtype is associated with epithelial-mesenchymal transition (EMT) and activation of *KRAS* and AKT pathways, and inflammatory signatures. BM1 tumors are aggressive and exhibit high phosphorylation levels of AKT and downstream targets such as 4EBP1, reflecting enhanced mTOR pathway activity.
- BM2 subtype is enriched for cell-cycle deregulation. These subtypes is characterized by increased CDK1 activity and low cyclin D1 expression. BM2 tumors demonstrate higher proliferation rates but less invasive potential compared to BM1. It exhibit distinct biological behaviors and therapeutic responses, underscoring the heterogeneity within *BRAFV600E*-mutated CRC.

In addition to the *BRAFV600E* mutation, metastatic cases frequently acquire co-mutations and genomic alterations that contribute to therapy resistance and disease progression. Common alterations include 53,61,62:

- *TP53* mutations: this alteration is found in up to 40-50% of *BRAF*<sup>V600Emut</sup> mCRC cases. *TP53* mutations result in loss of genomic stability, contributing to aggressive tumor behavior,
- *PIK3CA* mutations: occurring in 40–50% of *BRAF*<sup>V600Emut</sup> mCRC cases. These mutations activate the PI3K/AKT/mTOR signaling pathway, providing survival advantages. Alterations in *PIK3CA* gene contribute to resistance against MAPK pathway inhibitors and are potential targets for combination therapies,
- RAS pathway alterations *BRAF*<sup>V600Emut</sup> mCRC rarely co-occurs with *RAS* mutations (*KRAS* or *NRAS*), as these mutations are mutually exclusive. However, KRAS/NRAS activation through other mechanisms (e.g., feedback signaling) can contribute to resistance against *BRAF* inhibitors,
- Amplifications in *MET* and *ERBB2*: often occur as resistance mechanisms following MAPK-targeted therapies, such as *BRAF* and *MEK* inhibitors.

These alterations highlight the complexity of  $BRAF^{V600Emut}$  mCRC and the need for combination therapies targeting multiple pathways.

Clinically, *BRAF*<sup>V600Emut</sup> mCRC is more common in females and older adults, with a median age at diagnosis of over 60 years. These tumors predominantly occur in the right colon and often present at advanced stages, with high rates of peritoneal and lymph node metastases, exhibiting poor performance status (Eastern Cooperative Oncology Group [ECOG] 1–2)<sup>57,58,60</sup>. The metastatic pattern of *BRAF*<sup>V600Emut</sup> mCRC is unique compared to other CRC subtypes. Peritoneal carcinomatosis is a frequent finding, whereas lung metastases are relatively uncommon. This distinct metastatic profile often limits surgical options for curative resection, leading to reliance on systemic therapies<sup>63,64</sup>.

The prognosis of  $BRAF^{V600Emut}$  mCRC is significantly worse than that of BRAF wild-type cases, with

median overall survival (OS) typically less than 12 months without targeted therapy. The mutation serves as an independent negative prognostic marker and is associated with poor response to standard chemotherapy regimens, including 5-fluorouracil and oxaliplatin. The intrinsic resistance of  $BRAF^{V600Emut}$  tumors to conventional treatments emphasizes the need for novel therapeutic strategies and comprehensive molecular profiling in clinical practice. However, the prognosis varies with microsatellite instability status. MSI-positive tumors, enriched with immune infiltration, exhibit relatively better outcomes due to the anti-tumor immune response, while MSS tumors are associated with rapid disease progression and therapy resistance  $^{56-58,60}$ .

#### 1.2.3. Management of BRAFV600Emut mCRC

The management of BRAFV600Emut mCRC continues to evolve, driven by advancements in understanding tumor biology and treatment strategies. While recent developments in targeted therapies have improved patient outcomes, resistance mechanisms and treatment challenges persist. For patients diagnosed with BRAF<sup>V600Emut</sup> mCRC, the first-line treatment often involves combination chemotherapy. Regimens like FOLFOX or FOLFIRI, sometimes paired with bevacizumab, an antivascular endothelial growth factor (VEGF) agent, are commonly used. For patients with good performance status, the triplet regimen FOLFOXIRI, combined with bevacizumab, is preferred due to its higher response rates. However, these regimens are not without challenges. However, these regimens offer only limited control over the disease, with progression-free survival (PFS) of 4-6 months, and are associated with significant toxicity, especially in older or frail patients 48,63,65-68. When first-line treatments fail, the introduction of targeted therapies has provided a much-needed option. The BEACON CRC trial established a new standard of care with the combination of encorafenib, a BRAF inhibitor, and cetuximab, an EGFR inhibitor, in the second-line setting. This regimen demonstrated a significant improvement in overall survival (OS) compared to chemotherapy, increasing median OS to 8.4 months from 5.4 months. For some patients, adding binimetinib, a MEK inhibitor, to this combination can further improve outcomes, though at the cost of increased toxicity. While these therapies have been a breakthrough, resistance often develops within months, limiting their long-term effectiveness.

One of the most significant obstacles in managing  $BRAF^{V600Emut}$  mCRC is therapy resistance. Despite initial responses, tumors often progress within months due to their ability to activate alternative survival pathways. The mechanisms of resistance can be broadly classified into three categories  $^{64,66,68,69}$ :

- MAPK Pathway Reactivation: tumors frequently bypass *BRAF* inhibition by reactivating the MAPK signaling pathway through feedback loops. The most common mechanism involves

- upregulation of epidermal growth factor receptor (EGFR) signaling, which can restore downstream MAPK activity despite the presence of *BRAF* inhibitors,
- Activation of Alternative Pathways: in addition to reactivating MAPK, tumors can activate parallel survival pathways, such as the PI3K/AKT/mTOR axis. Alterations in *PIK3CA* or loss of *PTEN*, both of which enhance PI3K signaling, have been identified in resistant tumors. These changes allow tumor cells to continue proliferating despite targeted therapy,
- Genetic Heterogeneity and Tumor Evolution: the heterogeneous nature of *BRAF*<sup>V600Emut</sup> mCRC contributes to resistance. Subclonal populations within the tumor can harbor additional mutations, such as *KRAS* or *MET* amplifications, which drive resistance. These genetic changes often emerge under the selective pressure of targeted therapies.

Recognizing these resistance mechanisms, researchers are exploring new combinations of therapies to shut down the escape routes tumors use. For example, combining *BRAF/EGFR* inhibitors with agents targeting the PI3K or mTOR pathways is being studied to address the dual challenges of MAPK pathway reactivation and alternative pathway activation<sup>64,66</sup>. Similarly, adding antiangiogenic agents like bevacizumab to targeted therapies aims to disrupt the tumor's blood supply, potentially enhancing treatment efficacy.

Another promising avenue is combining targeted therapies with immune checkpoint inhibitors (ICIs). While ICIs like pembrolizumab have shown remarkable success in MSI-H tumors, their role in MSS tumors, which make up the majority of  $BRAF^{V600Emut}$  mCRC cases, has been limited. By pairing ICIs with targeted therapies, researchers hope to overcome the immune-evasive nature of MSS tumors and extend the benefits of immunotherapy to more patients  $^{64,66,68,70}$ .

Furthermore, current therapies largely address later stages of treatment, leaving an unmet need for effective first-line targeted options. While first-line regimens are currently limited to chemotherapy-based combinations, emerging evidence suggests that integrating targeted therapies earlier may improve outcomes. Trials are ongoing to evaluate the use of encorafenib and cetuximab, potentially in combination with chemotherapy or anti-angiogenic agents like bevacizumab, in the first-line setting <sup>68,70</sup>.

At the same time, efforts to expand access to molecular testing are crucial. Comprehensive profiling, including BRAF, MSI, and RAS status, is essential for guiding treatment decisions, yet testing remains inconsistent in some regions. Universal access to molecular diagnostics is a critical step toward ensuring all patients receive the most effective, personalized care<sup>63,69</sup>.

One of the most exciting developments in managing  $BRAF^{V600Emut}$  mCRC is the use of liquid biopsies. These non-invasive tests detect ctDNA in the blood, offering a window into the genetic evolution of the tumor in real time. By identifying emerging resistance mutations early, liquid biopsies enable

clinicians to adapt therapies before the tumor progresses. This approach has the potential to make treatment more dynamic and personalized, addressing resistance as it arises rather than reacting to it after progression<sup>63</sup>.

While recent advancements have improved outcomes for many patients, significant challenges remain. Resistance to targeted therapies, variability in tumor behavior, and the need for better first-line options highlight the complexity of managing this disease.

#### 2. AIMS

BRAF-V600E mCRC represents about 12% and is linked to a particularly poor prognosis. Even with advancements in precision oncology and targeted therapies like Cetuximab combined with Encorafenib—as highlighted in the BEACON study, outcomes for these patients remain grim. Median overall survival is just 4 to 6 months after initial treatments fail, and many patients do not respond to BRAF inhibitors despite the presence of the target mutation. This suggests that there are still many unknowns about resistance mechanisms, which limits the potential for better outcomes.

The BRAF-V600E-Mutated colorectal cAncer: primary and acquired reSistanCe to tArgetedtReAtment study (MASCARA project) is designed to tackle these challenges. The goal is to understand why some patients with *BRAF V600E* mCRC don't respond to targeted treatments, and what biological processes might be driving both primary and acquired resistance. By shedding light on these mechanisms, the study aims to open up possibilities for improving treatment options and survival rates for this difficult-to-treat group of patients.

The primary objective of the MASCARA project focuses on identifying primary resistance mechanisms to chemotherapy in *BRAF V600E* mCRC patients. Molecular analyses, including whole-exome sequencing (WES) and the Nanostring GeoMx® Digital Spatial Profiler (DSP), will be conducted on Formalin-Fixed Paraffin-Embedded (FFPE) samples to identify resistance pathways and mechanisms. For the secondary aim, the project will investigate circulating biomarkers of acquired resistance through longitudinal analysis of plasma samples from prospective patients. Circulating cell-free DNA (cfDNA) extracted from plasma will be analyzed using next-generation sequencing (NGS) on the Illumina platform to evaluate a large gene panel. All molecular analyses will be carried out at the Laboratorio di Bioscienze of IRCCS IRST in Meldola, Italy. Additionally, the correlation between imaging data and the clinical and biological characteristics of patients will be explored to provide further insights into resistance mechanisms.

This project is all about improving the way we treat patients with *BRAF V600E* mCRC. By understanding why some patients do not respond to existing therapies and finding better ways to predict and tackle resistance, we can take a step closer to truly personalized cancer care. The findings could also pave the way for new treatment targets, offering hope for better survival and quality of life for patients who currently face very limited options.

#### 3. PATIENTS AND METHODS

# 3.1 BRAF-V600E-Mutated colorectal cAncer: primary and acquired reSistanCe to tArgetedtReAtment (MASCARA project)

The MASCARA project, conducted as part of the "Integrated Multiomics and Multilevel Characterization in Colorectal Cancer (MiMiC)" exploratory study, represents a comprehensive, multicenter (IRCCS IRST, AVR, the University of Pisa, IRCCS INT of Milano, the University of Vita-Salute San Raffaele of Milano, and AOU Modena), exploratory, non-pharmacologic, observational, translational study. The study was approved by the Local Ethics Committees of each center and informed consent was obtained from each patient for their biological material to be used for research purposes. The project is designed to enhance our understanding of resistance mechanisms in *BRAFV600E* metastatic colorectal cancer (mCRC) patients treated with the combination of Encorafenib and Cetuximab (Figure 13).

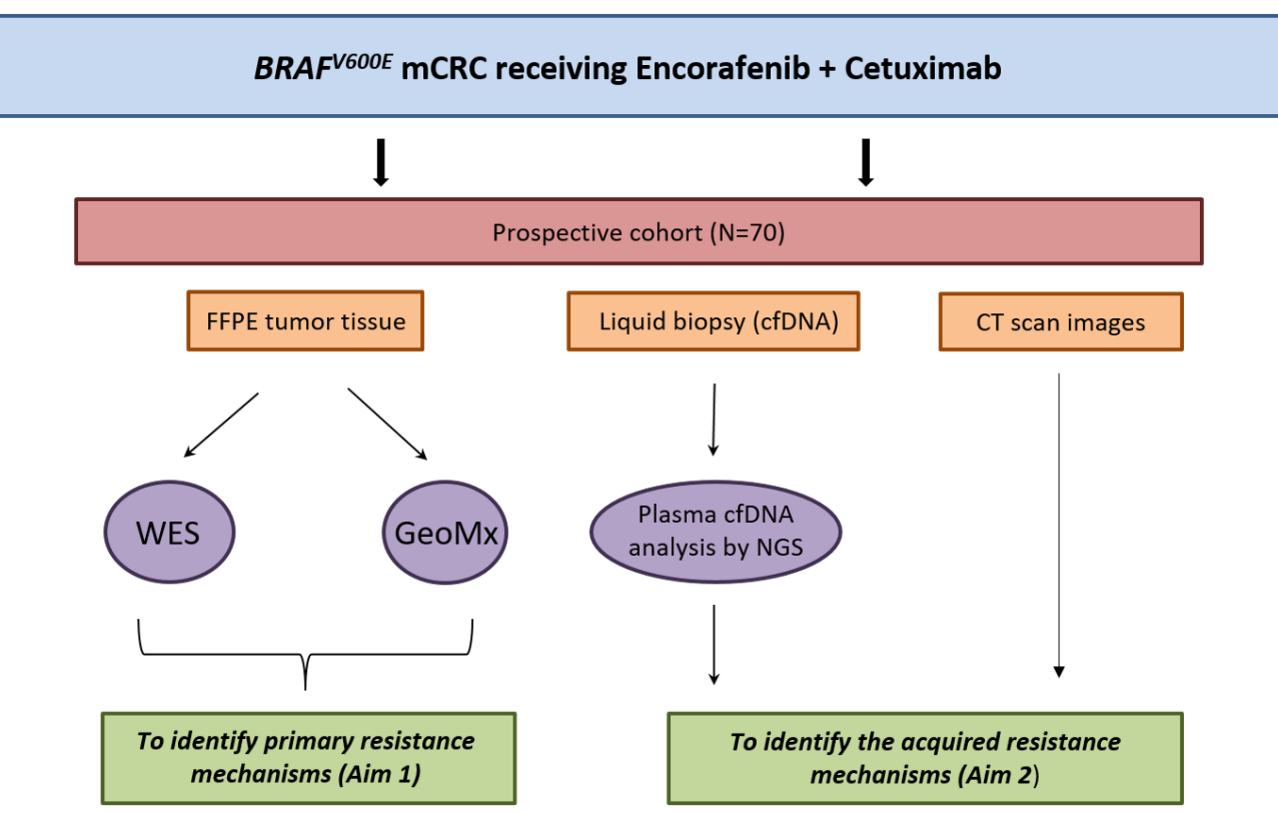


Figure 13. Graphical abstract of MASCARA project.

#### 3.2 Patient enrollment

All centers involved in MASCARA study have an active role in patient enrollment. The entire case series of MASACRA project consists of 70 patients. Data and samples were collected from patients whose tumor tissues were obtained between July 2021 and December 2024 and stored at the U.O. of Anatomia Patologica. These formalin-fixed-paraffin-embedded (FFPE) samples will be instrumental

for addressing the primary objectives of the study. In addition, a second group of patients who provided specific informed consent will be included, utilizing plasma samples collected at baseline and during follow-up, which are stored at the Biological Resource Center of IRCCS IRST. These plasma samples will contribute to achieving the secondary objectives.

The main inclusion criteria for the study include a signed and dated informed consent document, age of 18 years or older at the time of consent, histologically or cytologically confirmed mCRC with the presence of the BRAF V600E mutation as determined by local PCR or NGS assays, progression of disease after one or two prior metastatic regimens, measurable or evaluable non-measurable disease by RECIST v1.1 criteria, an ECOG performance status of 0 or 1, adequate bone marrow, renal, and hepatic function, and the ability to take oral medications. Treatment regimens consist of Cetuximab administered as a 400 mg/m2 initial dose on Cycle 1 Day 1, followed by 250 mg/m2 weekly, and Encorafenib administered daily at a dose of 300 mg (four 75 mg oral capsules).

#### 3.3 DNA isolation from FFPE tissue samples

The automated DNA isolation process was conducted from 30 FFPE samples, using Maxwell® RSC DNA FFPE Kit (Promega Corporation, Madison, WI, USA). The procedure was carried out according to the manufacturer's protocol, with minor modifications as described below. FFPE tissue blocks were sectioned into slices of 5-10 µm thickness using a microtome. Approximately 3-5 sections per sample were collected in a 1.5 mL microcentrifuge tube. To remove paraffin, 1 mL of xylene was added to the tube, followed by vigorous vortexing for 30 seconds. Samples were centrifuged at 14,000 x g for 2 minutes, and the supernatant was discarded. The deparaffinization step was repeated to ensure complete removal of paraffin. Residual xylene was removed by washing the pellet twice with 1 mL of 100% ethanol. The samples were air-dried for 10-15 minutes to eliminate ethanol traces. The dried tissue pellet was resuspended in 300 µL of lysis buffer (provided in the kit) containing Proteinase K (40 µL). The mixture was incubated at 70°C for 1 hour with intermittent vortexing to facilitate complete tissue digestion. Following this, the sample was cooled to room temperature before proceeding to the DNA extraction step. The lysate was transferred into a cartridge provided with the Maxwell® RSC DNA FFPE Kit. Each cartridge was preloaded into the Maxwell® RSC instrument along with elution tubes containing 50 µL of elution buffer. The Maxwell® RSC instrument was programmed to run the "DNA FFPE" method, which automates the binding, washing, and elution steps of DNA isolation. The process required approximately 45 minutes to complete. The eluted DNA was collected in the elution tubes and quantified using The samples were stored at -20°C until further analysis.

#### 3.4 Whole-Exome Sequencing (WES)

WES specifically analyzes only the exome, the coding portions of the genome, and enables the detection of a broad range of mutations, providing insights into genetic alterations in cancer. Through this sequencing approach, it is possible to study genetic variants in the human genome, which may help identify potential genetic factors responsible for the pathogenesis of diseases such as cancer. WES was performed for 30 samples of case series, using the Illumina next-generation sequencing

WES was performed for 30 samples of case series, using the Illumina next-generation sequencing (NGS) platform to analyze tumor tissue. For greater accuracy, when available, DNA from normal tissue was extracted and analyzed to create a bioinformatics baseline. The first step in exome generation involved library preparation, requiring approximately 100 ng of genomic DNA extracted from both tumor tissue and blood. DNA quantification was performed using a fluorometric method with the Qubit<sup>TM</sup> dsDNA Quantification Assay kit, measured on the Qubit fluorometer (ThermoFisher Scientific). Following this, the Illumina DNA Prep with Exome 2.4 Enrichment Kit (Illumina) was used for library synthesis. The library preparation protocol for exome sequencing consists of two main steps: 1) Library preparation via tagmentation on microspheres followed by amplification, and 2) Exome enrichment through hybridization-capture. Tagmentation involves enzymatic fragmentation of the DNA, simultaneously attaching adapter sequences to the fragment ends using transposons bound to microspheres. The fragmented DNA is then amplified by incorporating index sequences into the adapters, which are essential for sample recognition, and generating the genomic DNA libraries. These libraries were pooled in sets of 12 samples and underwent exome capture by hybridizing with biotinylated probes specific to the coding regions, approximately 35 Mb of the genome (Figure 14).

Exome sequencing offers the advantage of focusing solely on the exonic portions of the genome, enabling the identification of approximately 85% of mutations, including single nucleotide variants and small insertions or deletions (indels). After library preparation, the exome libraries were quantified using Qubit and their size assessed through capillary electrophoresis on the Agilent Bioanalyzer 2100. The concentration, expressed in nM, was determined using the following formula:

Concentration (nM) = 
$$(ng/\mu L) \times 660 \times 10^6 / (bp) \times 1000$$

The library pools were then normalized to the same nM concentration and loaded onto the Novaseq6000 sequencer (Illumina), in paired-end mode ( $150 \text{ bp} \times 2$ ).

An important parameter for data quality and analysis is coverage, which refers to the number of times a base in the reference sequence, particularly coding regions, is covered by sequencing reads. For this study, the samples were sequenced to achieve a theoretical coverage of greater than 150X for the tumor greater than 50X for the germline samples. The sequencing data were then analyzed by the bioinformatics team at the IRST IRCCS using dedicated bioinformatics pipelines.

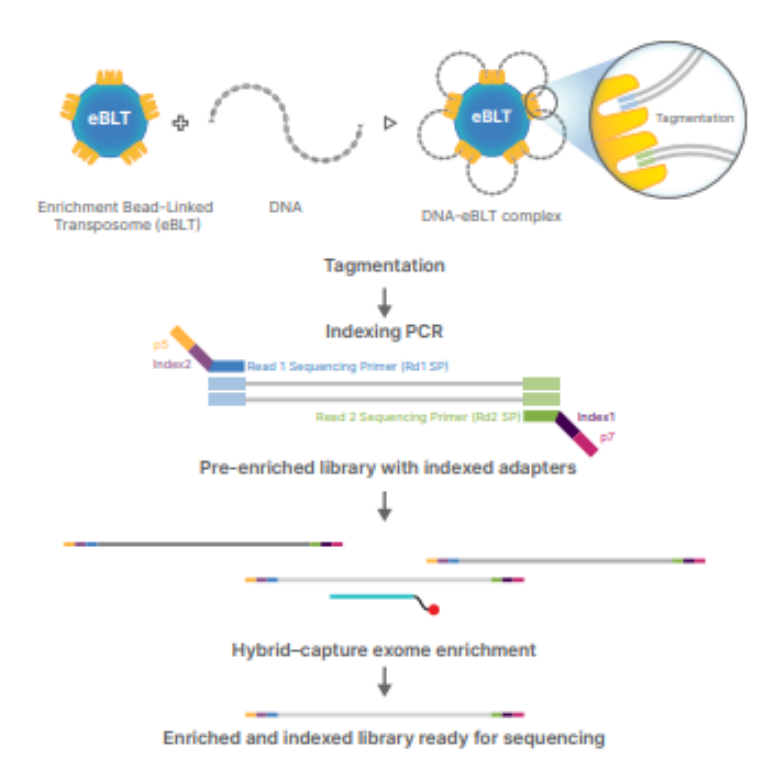


Figure 14. **Streamlined tagmentation-based library preparation with exome enrichment.** Enrichment bead-linked transposomes (eBL) facilitate a consistent tagmentation process with robust tolerance to varying DNA input amounts. Following hybrid-capture enrichment, exome libraries are prepared for sequencing.

#### 3.5 Circulating tumor DNA (ctDNA) isolation from plasma samples

The isolation of circulating tumor DNA (ctDNA) from plasma samples was performed using the QIAamp® Circulating Nucleic Acid Kit (Qiagen, Hilden, Germany). Peripheral blood samples were collected in EDTA-coated vacutainer tubes to prevent clotting. Blood was centrifuged at  $1,900 \times g$  for 10 minutes to separate plasma from cellular components. The plasma supernatant was carefully transferred to fresh tubes, avoiding disruption of the buffy coat layer. A second centrifugation step was performed at  $16,000 \times g$  for 10 minutes to remove any remaining cellular debris. The cleared plasma was aliquoted into 1 mL fractions and stored at -80°C until ctDNA extraction.

Plasma samples (1-2 mL) were thawed on ice and mixed with 1 volume of proteinase K (provided in the kit) and 4 volumes of Buffer ACL containing carrier RNA. The mixture was vortexed briefly to ensure homogeneity. The lysate was incubated at 60°C for 30 minutes to enhance lysis and ctDNA release. After lysis, 1 volume of ethanol (100%) was added to the mixture to facilitate binding of nucleic acids to the silica membrane. The lysate-ethanol mixture was transferred to the QIAamp Mini column placed in a 2 mL collection tube. The columns were centrifuged at  $6,000 \times g$  for 1 minute, and the flow-through was discarded. This step was repeated for the entire lysate volume. The silica membrane was washed sequentially with  $600 \mu L$  of Buffer ACW1, followed by  $750 \mu L$  of Buffer ACW2. Each washing step included centrifugation at  $6,000 \times g$  for 1 minute to remove contaminants.

A final drying step was performed by centrifuging the column at  $16,000 \times g$  for 3 minutes to eliminate residual ethanol. The QIAamp Mini column was placed in a clean 1.5 mL microcentrifuge tube, and 50  $\mu$ L of Buffer AVE (elution buffer) was added directly to the center of the silica membrane. After a 5-minute incubation at room temperature, the column was centrifuged at  $6,000 \times g$  for 1 minute to collect the purified ctDNA. ctDNA yeld was determined with Qubit fluorometer (ThermoFisher Scientific). Quality and integrity assessment was evaluated through 2100 Bioanalyzer (Agilent).

# 3.6 TruSight<sup>TM</sup> Oncology 500 ctDNA

As of now, we collected blood samples (plasma and buffy coat) from 17 patients enrolled in the trial. The TruSight Oncology 500 ctDNA kit (Illumina) was employed on the NovaSeq 6000 platform to analyze plasma samples collected from 12 patients at baseline (CT01) and additionally from 8 of these patients at disease progression (CT02).

TSO 500 ctDNA represents a cutting-edge approach to comprehensive genomic profiling for precision oncology, enabling the detection of key biomarkers across various cancer types through the analysis of circulating tumor DNA. At its core, TSO 500 ctDNA focuses on detecting single nucleotide variants (SNVs), insertions and deletions (indels), copy number variants (CNVs), and genomic rearrangements, while also providing insights into microsatellite instability (MSI) and tumor mutational burden (TMB), both critical markers for immunotherapy response. The extracted cfDNA (30 ng) undergoes library preparation involving hybrid capture-based enrichment, specifically targeting 523 genes associated with oncology. This ensures a focused yet comprehensive analysis, amplifying the regions of interest while reducing background noise. In the TSO 500 ctDNA protocol, Unique Molecular Identifiers (UMIs) are used to improve the accuracy and reliability of sequencing data. UMIs are short, random sequences of nucleotides added to individual DNA fragments during library preparation. UMIs help distinguish true biological variants (mutations) from sequencing or PCR errors. Since each DNA molecule is tagged with a unique sequence, any errors introduced during amplification or sequencing can be identified and corrected by comparing reads with the same UMI. Following library preparation, the samples are sequenced using the Illumina NovaSeq6000 platform, at 150 bp paired end. An average coverage of 1300X of the target region was obtained in all samples. Sequencing data were processed and analysed with the DRAGEN TSO 500 ctDNA Analysis Software v2.1.1 (DRAGEN software version 3.10.9, Illumina) for the detection of single nucleotide variants (SNVs), InDels, copy-number variants (CNVs), gene fusions, and tumor mutational burden (TMB). Germline and intronic/intergenic variants were excluded from the analysis. Somatic SNVs were identified by the software and annotated on COSMIC and ClinVar (Figure 15). Variant allele frequency (VAF) was of somatic mutations was used as an estimation of the fraction of tumor DNA present in the plasma.

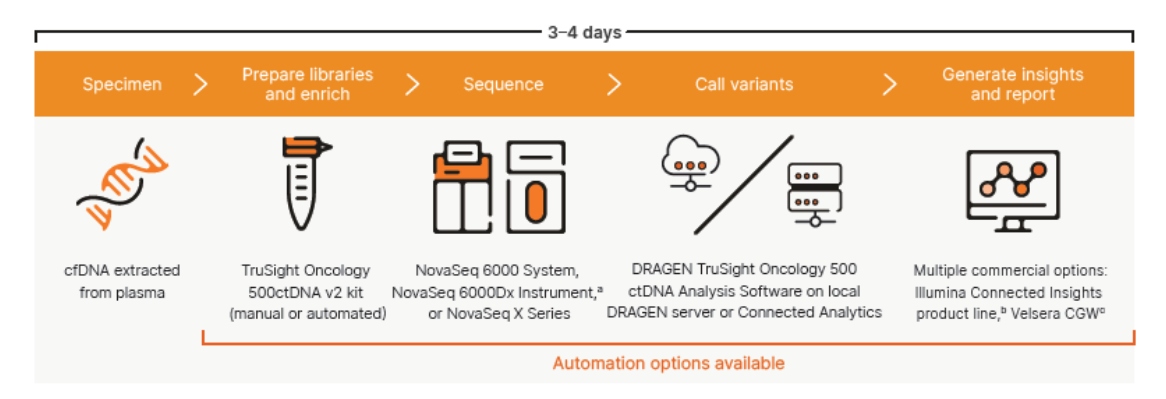


Figure 15. **Workflow for TruSight Oncology 500 ctDNA testing**, outlining the key steps from cfDNA extraction to insights generation. The process includes specimen preparation, library enrichment using the TruSight Oncology 500 ctDNA v2 kit, sequencing on NovaSeq 6000 systems, variant calling with DRAGEN TruSight Oncology 500 ctDNA Analysis Software, and data reporting with commercial tools such as Illumina Connected Insights.

## 3.7 NanoString GeoMx® Digital Spatial Profiler

In a selected subset of a case series of nearly 10 patients (paired as 5 responders and 5 nonresponders), we will performed an innovative method of transcriptomic analysis using the Nanostring GeoMx® Digital Spatial Profiler (DSP). GeoMx DSP was employed to evaluate RNA expression levels within colorectal cancer samples, focusing on differentiating responder and non-responder tumor and tumor microenvironment (TME) characteristics. This cutting-edge spatial profiling platform integrates classical histological staining with multiplexed molecular quantification, enabling high-resolution spatial analysis of biomarker expression. In this study, tissue samples were obtained from patients diagnosed with colorectal cancer, FFPE sections were utilized to ensure structural integrity and molecular stability. For selected cases, we performed immunohystochemical staining for BRAFV600E mutation and EGFR expression, to evaluate interesting region of intratumoral heterogeneity. Moreover, we performed classical staining protocols included the nuclear dye Syto13 to define cellular architecture, anti-CD45 antibody for pan-leukocyte detection, and antipancytokeratin antibody to identify epithelial tumor regions. These markers were chosen to delineate distinct compartments of the tissue: tumor regions, immune cell populations, and overall stromal contributions. Regions of interest (ROIs) were selected to represent tumor and TME areas for subsequent profiling. Responders and non-responders were categorized based on clinical outcomes, particularly therapeutic response rates and progression-free survival metrics. The profiling involved labeling tissue sections with oligonucleotide-barcoded antibodies specific to a panel RNA targets, followed by imaging to capture spatial context. The hybridization signals from the barcoded probes were digitally quantified using the NextSeq 550 Illumina sequencer and DCC creation files. The resulting data were then deconvoluted, yielding a spatially resolved molecular profile. Data normalization and batch correction were applied to mitigate technical variability, with expression levels compared between responders and non-responders to identify differential biomarker patterns (Figure 16).

This approach enabled a comprehensive understanding of tumor biology and immune infiltration patterns, elucidating key differences between patient groups and highlighting potential therapeutic targets.

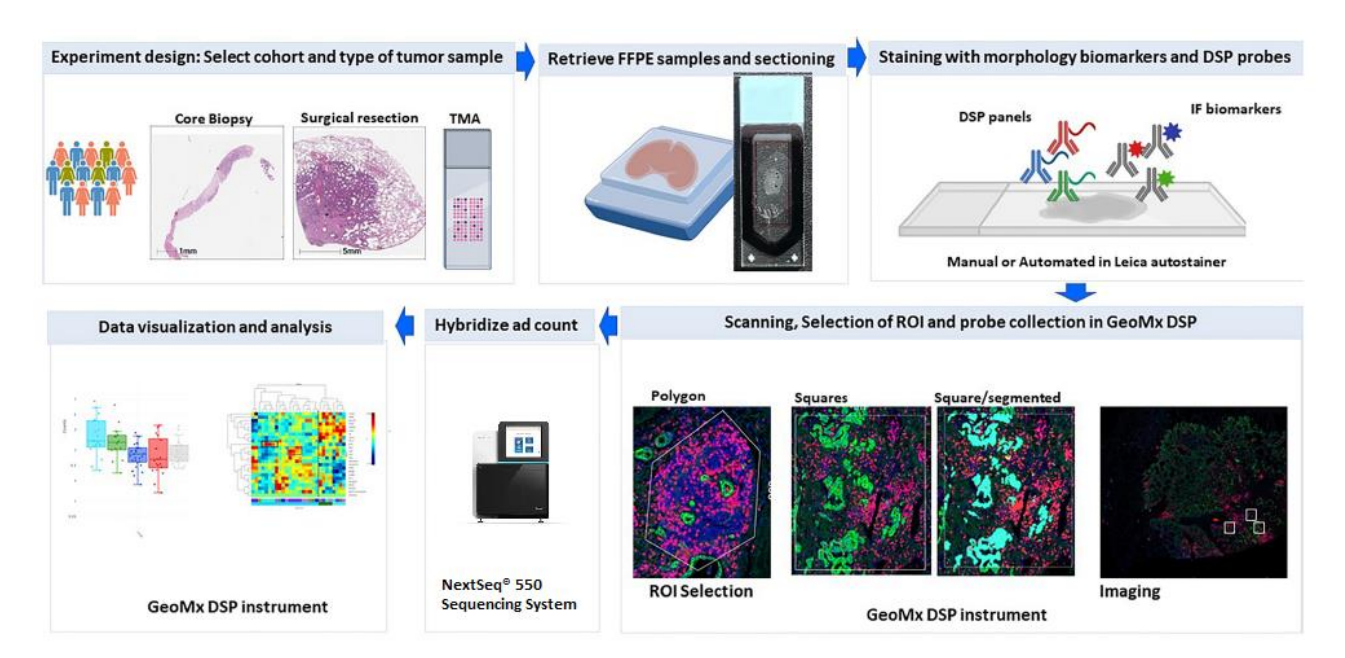


Figure 16. **GeoMx DSP workflow.** Illustration showing the procedural steps involved in profiling with the GeoMx DSP.

# 3.8 Bioinformatical analysis

Exome analysis was conducted using the DRAGEN tumor-only pipeline designed to identify SNV, indel, MSI and TMB. To minimize artifacts caused by systematic noise, such as mismatch in low-complexity regions or PCR artifacts in homopolymer regions, the analysis used a specific baseline constructed from the germline DNA of 60 patients with clinical features similar to those of the study cohort and prepared using the same approach.

The main steps of the analysis included: converting BCL files (the output of the sequencing platform) to FASTQ format, mapping and aligning reads to the GRCh38 reference genome, sorting, marking duplicates, and variant calling for variant identification.

Variants detected in VCF files were annotated using ANNOVAR and VarSome, and then filtered with custom scripts in order to identify somatic variants.

The following filters were applied:

- Variants located in exonic or splicing regions;
- Variants supported by at least five reads;
- Variants with a population frequency of less than 0.01 or absent from the Genome Aggregation Database (gnomAD);
- Variants that pass DRAGEN quality filters;
- Variants annotated by VarSome, based on ACMG guidelines, as variants of uncertain significance (VUS), probably pathogenic or pathogenic;
- Variants classified by VarSome, based on AMP guidelines, as Tier I, II, or III;
- Variants annotated as somatic or without any annotation in the Nirvana database.

To identify the most frequently mutated genes within the cohort, the following criteria were applied:

- Synonymous variants were excluded.
- Genes classified as pseudogenes or highly polymorphic were excluded unless they were annotated as oncogenes, tumor suppressors, or listed among genes relevant to the pathology <sup>71</sup>;
- Genes were required to harbor a variant in at least five samples, or in at least two samples for genes included in the pathology-related list.

The selected cutoff values were > 1 mut/Mb to define high TMB and >20% of unstable microsatellite sites to define MSI. The OncoPrint were generated using the ComplexHeatmap R package.

For Trusight Oncology 500 ctDNA data were analyzed using the Illumina TSO500 Local App software version 2.1.0 for the analysis of small variants, TMB, MSI status, copy number variation (CNV), and DNA fusions starting from BCL files. Specific bioinformatic filters were applied to refine variant selection and ensure clinical relevance. Variants classified as "germline DB" were excluded, as these represent polymorphisms present in various databases of healthy populations, typically with an allele frequency exceeding 1%. Synonymous and intronic variants were also eliminated to focus on alterations with potential functional impact. Furthermore, variants predicted by the Varsome platform to be benign or likely benign were systematically excluded, as they are unlikely to contribute to the pathogenic landscape. This rigorous filtering process ensured a precise and meaningful dataset for downstream analyses.

Finally, for spatial transcriptomic analysis, the sequencing FASTQ files were processed using the GeoMx® NGS Pipeline to generate DCC files compatible with the GeoMx DSP Analysis Suite. Subsequently, these DCC files were analyzed using the GeoMx DSP Analysis Suite, which involved conducting data quality control, filtering, normalization, and differential expression analysis. During the data quality control phase, the reads from all 15 ROIs were evaluated based on several criteria: the percentage of raw reads aligned (threshold set at 80%), sequencing saturation (threshold set at 50%), the geometric mean of negative probe counts (threshold set at five counts), and the minimum

nuclei count (threshold set at 200 nuclei). Consequently, 1 ROIs were identified with a negative probe count geometric mean below 5. Probe quality control (QC) was also conducted, and probes that failed to meet the following criteria: (geometric mean of the probe in all ROIs) / (geometric mean of probes within the target)  $\leq 0.1$  and failed Grubbs' outlier test in at least 20% of ROIs were excluded from target count calculations. Subsequently, AOI and target filtering steps were performed. For ROI filtering, any ROIs with fewer than 5% of targets exceeding the default expression threshold (higher of the limit of quantification [LOQ] or a user-defined value of 2) were removed. Similarly, target filtering was applied, removing any targets present in less than 3% of AOIs from further analysis. After completing the quality control and filtering processes, 865 genes were excluded, resulting in a final dataset comprising 947 genes and 15 ROIs, which was used for downstream analyses. Following this, the raw count data were normalized using the Q3 normalization method. To assess the changes in expression between tumor and TME compartments, a linear mixed model analysis was conducted using the GeoMx DSP Analysis Suite. Volcano plots displaying the results were generated with the GeoMx Analysis Suite plugin, Volcano Plot. Significant results were defined by a fold-change cutoff of 1.5 and a p-value  $\leq$  0.05. Finally, a functional pathway analysis was performed using the DSP software, and a dot blot was created with the SRPlot tool. Pathways with significant enrichment were identified based on a p-value  $\leq 0.05$ .

#### 4. RESULTS

### 4.1 Patient characteristics

In the MASCARA study, a total of 50 patients have been enrolled to date. Of the entire cohort, the main clinical characteristics of 30 patients have been retrieved and are summarized in Table 2. The median age at diagnosis is 69 years, with a higher incidence in females (70%). The primary tumor is located in the right colon in 80% of cases. All patients have metastases, sometimes involving multiple organs, with hepatic (40%) and pulmonary (30%) metastases being the most frequent.

At the beginning of treatment with Encorafenib plus Cetuximab, 76.7% of patients had an ECOG performance status of 1. Microsatellite instability (assessed through Next-Generation Sequencing panel during the diagnostic process) is present in 20% of the cohort. Finally, the response to treatment (according to RECIST criteria v1.1) was categorized into Responders (R) and Non-Responders (NR). Patients classified as "Non-Responders" include those with stable disease (SD) as the best response to treatment and those with progressive disease (PD) at the first reassessment, constituting 80% of the cohort. In contrast, "Responders" include patients with complete response (CR) and partial response (PR), representing 20% of the cases.

Clinico-pathological features	Total (n=30) N. (%)
Age at diagnosis: median age (range)	69 (50-83)
Gender Male Female	9 (30) 21 (70)
<b>Primitive tumor location</b> Right Left	24 (80) 6 (20)
ECOG 0 1 2	5 (16.6) 23 (76.7) 2 (6.7)
Metastasis site Liver Lung Peritoneum Node Bone Retro-peritoneum	12 (40) 9 (30) 16 (53.3) 10 (33.3) 3 (10) 1 (3.3)

#### **MSI** status

MSS	24 (80)
MSI-H	6 (20)
<b>D</b> • • • • •	
Previous treatment	
FOLFOX	3 (10)
FOLFOX plus Bevacizumab	3 (10)
FOLFIRI	2 (6.7)
FOLFIRI plus Aflibercept	4 (13.3)
FOLFOXIRI	2 (6.7)
FOLFOXIRI plus Bevacizumab	3 (10)
CAPOX	4 (13.3)
CAPOX plus Bevacizumab	2 (6.7)
XELOX	2 (6.7)
TOMOX	1 (3.3)
Capecitabine	4 (13.3)
Response to Encorafenib+Cetuximab	
Responder (CR+PR)	6 (20)
•	
Non-responder (PD+SD)	24 (80)

Table 2. Clinico-pathological characteristics of case series. Abbreviation: Microsatellite instability (MSI-H), Microsatellite stability (MSI-L), Complete Response (CR), Partial Response (PR), Stable disease (SD), Progression disease (PD)

### 4.2 WES data analysis

The mutational profile of the 30 baseline FFPE samples is summarized in the Oncoprint chart (Figure 17), showing alterations across multiple genes and stratified by classification groups (R: responder, NR: non-responder), tumor mutational burden (TMB-high and TMB-low), and microsatellite instability (MSI-H and MSS). The analysis confirmed the presence of BRAFV600E mutation in all patients of the cohort. Moreover, the most frequently mutated genes across all samples were: TP53 mutations occur in 60% of patients, primarily through missense variants (53%), followed by splicing variants (24%). BRINP3 mutations are found in 40% of patients, predominantly through missense variants (92%). CHSY3, RNF43, and SMAD4 mutations are observed in 27% of patients, with missense variants and frameshift indels being the primary types of mutations. The remaining genes showed in Figure 17 demonstrate mutation frequencies ranging from 23% down to 7%. Across all genes, missense variants were the most common type of alteration observed, followed by frameshift indels and nonsense variants. Less frequent mutation types included splicing variants, start loss, stop loss, and inframe indels. The classification of patients based on MSI and revealed that 24 patients (80%) are MSS and 6 patients (20%) are MSI-H. While, the majority of the cohort (87%) present TMB-H and only 13% of cases show a TMB-L. All MSI-H patients are TMB-H. Furthermore, the 50% of MSI-H present alterations in *PLEC* and *PI3KCA* genes.

It is observed that *NOTCH3*, *LRP2*, *FBXW7*, *FAT1*, *CREBBP*, *PTEN*, *KMT2B*, *UBC*, *PI3KCA*, *CTNNA3*, *ABCC6*, *ANK3* and *TGFBR2* were exclusively mutated in NR patients. Conversely, no genes were exclusively mutated in R patients. Finally, it is noted that 83% (5/6) of MSI-H and 75% (3/4) of TMB-L are NR, respectively.

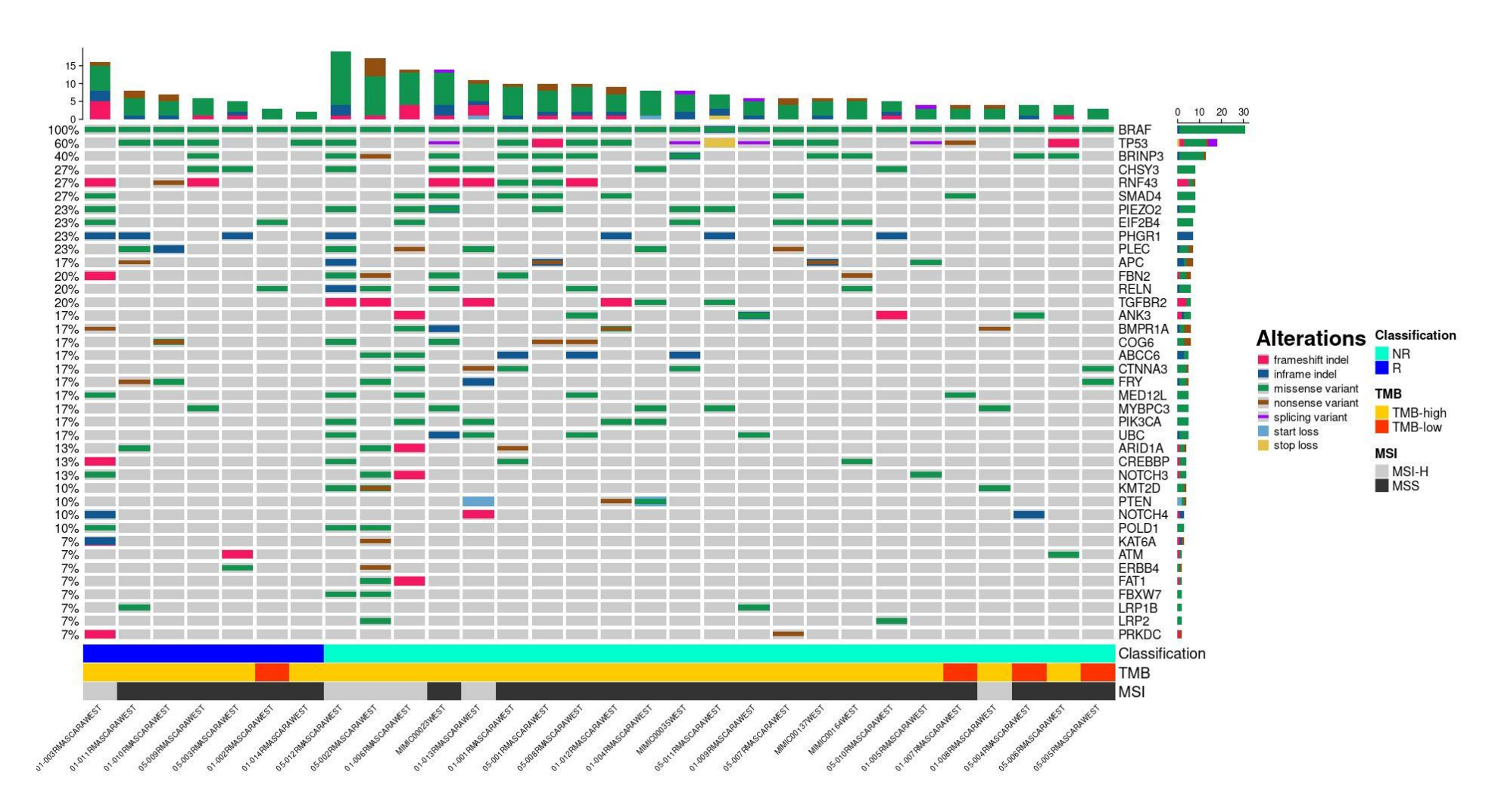


Figure 17. **The Oncoprint chart of WES data.** The Oncoprint chart shows the most significant pathogenic somatic mutations identified on FFPE tumor tissue (R, responders; NR, Non responders). To select the genes for visualization, we included those with at least three mutated samples as well as those known to be driver genes in colorectal cancer.

## 4.3 Liquid biopsy data analysis

The analysis of ctDNA at baseline (CT01) and at progression of disease (CT02) from eight patients revealed notable findings, summarized in the Oncoprint chart (Figure 18), stratified by treatment response (NR, R). A comparison between mutations identified in liquid biopsy at CT01 and those found in tumor tissue via whole exome sequencing (WES) showed complete concordance for the genes BRAF, PIK3CA, RNF43, NOTCH3, PRKDC, MAP2K1, and POLD1. For TP53, ATM, and APC genes, mutations detected in liquid biopsy were not identified by WES analysis of tumor tissue. Conversely, mutations in ARID1A, SMAD4, APC, and NOTCH4 genes were found only in the WES analysis of the tissue samples and not in ctDNA. The most frequently mutated genes were TP53 (56%), PIK3CA (56%), ARID1A (38%), RNF43 (38%), and SMAD4 (31%). Notable alterations emerged during disease progression (CT02), including mutations in PIK3CA (e.g., in CRC11 patient), TP53 (e.g., CRC06), ATM (e.g., CRC06), ARID1A (e.g., CRC13, CRC03), and KRAS (e.g., CRC06, CRC03). In contrast, mutations in SMAD4 and PTEN were exclusively present at CT01 in two patients (CRC04, CRC06). Of particular interest, four patients (CRC01, CRC06, CRC11, and CRC14) showed the emergence of a new mutation in BRAF, in addition to the V600E mutation, at disease progression. Certain genes, including PIK3CA, SMAD4, ATM, PTEN, APC, MAP2K1, and NOTCH4, exhibited mutations predominantly or exclusively in NR patients, while PRKDC and *POLD1* mutations were found only in R patients.



Figure 18. **Oncoprint chart of TSO500 ctDNA analysis.** In Figure we summarizes the most frequently mutated genes on plasma cfDNA. For gene visualization we select genes present both in WES and in TSO500 panel. Two plasma time points were selected for each patient (CT01: before treatment; CT02: at PD).

Figure 19 depicts the variant allele frequencies (VAF) of the analyzed genes. Notably, in patient CRC06, the emergence of distinct mutations is observed during disease progression in genes that were already mutated at the baseline time point. Additionally, Figure 20 specifically illustrates the VAF trend of the BRAFV600E mutation in patients analyzed using the TSO500 panel at time points CT1 and CT2, stratified by R and NR status. Among the NR patients, two patients exhibited a decrease in VAF at CT2 (01-001: CT1 = 0.5206, CT2 = 0.1383; 01-004: CT1 = 0.3906, CT2 = 0.1768), whereas three patients showed an increase in VAF at the PD time point (01-012: CT1 = 0.0483, CT2 = 0.2784; 01-013: CT1 = 0.0106, CT2 = 0.0146; 01-006: CT1 = 0.009, CT2 = 0.0164). In contrast, all R patients demonstrated a decline in BRAFV600E VAF between CT1 and CT2 (01-011: CT1 = 0.3148, CT2 = 0.2152; 01-014: CT1 = 0.226, CT2 = 0.1388; 01-003: CT1 = 0.0385, CT2 = 0.018).

								Patient	:ID							
	CRC01 CRC03		CRC04 CRC06		CRC11		CRC12		CRC13		CI	RC14				
	Ct01	Ct02	Ct01	Ct02	Ct01	Ct02	Ct01	Ct02	Ct01	Ct02	Ct01	Ct02	Ct01	Ct02	Ct01	Ct02
BRAF (VAF)	V600E (0.1383)	V600E (0.5206)	V600E (0.018)	V600E (0.0385)	V600E (0.0164)	V600E (0.009)	V600E (0.1768)	V600E (0.3906)	V600E (0.2152)	V600E (0.3148)	V600E (0.2784)	V600E (0.0483)	V600E (0.0146)	V600E (0.0106)	V600E (0.1388	V600E ) (0.226)
PIK3CA (VAF)	wt	wt	wt	wt	R88Q (0.0076) H1047R (0.0058)	R88Q (0.0072) H1047R (0.0053)	R88Q (0.1832)	R88Q (0.3528) H1047R (0.0071) V346E (0.0872) H1047Y (0.0112)	wt	R88Q (0.007)	R88Q (0.198)	R88Q (0.0512)	H1047R (0.0106)	H1047R (0.0055)	wt	wt
TP53 (VAF)	G112D (0.0911)	G112D (0.3584)	wt	wt	wt	wt	wt	R114C (0.0088) C137F (0.0059)	M114K (0.5601)	M114K (0.7204)	R116W (0.2198)	R116W (0.0403)	wt	wt		Y181S ) (0.0102)
ARID1A (VAF)	wt	wt	wt	D1850Gfs*4 (0.0154)	wt	wt	p.(Pro146GinfsTer86) (0.3125) P1468Lfs*13 (0.1481)	p.(Pro146GInfsTer86) (0.4583) P1468Lfs*13 (0.3523) P1326Rfs*155 (0.0101)	p.(Asp1231Val) (0.1946) p.(Cys1723TrpfsTer4) (0.5696)	p.(Asp1231Val) (0.1211) p.(Cys1723TrpfsTer 4) (0.7536)	wt	wt	wt	Q1519fs*8 (0.0091)	wt	wt
NOTCH3 (VAF)	wt	wt	p.(Gly2035ValfsTer50) (0.0117)	p.(Gly2035ValfsTer50 ) (0.0184)	wt	wt	p.(Leu2092TrpfsTer57) (0.1878)	p.(Leu2092TrpfsTer57) (0.3251) p.(Ala1802GlyfsTer8) (0.0085) p.(Ala1651Thr) (0.0166) p.(Leu1519Pro) (0.02) p.(Glu668Lys) (0.026)	wt	wt	wt	wt	wt	wt	wt	wt
RNF43 (VAF)	p.(Trp15Arg) (0.0656)	p.(Trp15Arg) (0.2666)	R117fs*41 (0.0215)	R117fs*41 (0.0583)	wt	wt	R117fs*41 (0.337)	R117fs*41 (0.7122)	wt	wt	wt	wt		R117fs*41 (0.0103) p.(Pro441LeufsTer61) (0.0084) p.(Arg117ThrfsTer41) (0.0059)	wt	wt
SMAD4 (VAF)	G386D (0.0641)	G386D (0.2512)	wt	wt	wt	wt	D52fs (0.0089) p.(Arg87Trp)(0.0094)	wt	wt	wt	E330Q (0.1931)	E330Q (0.0415)	wt	wt	wt	wt
CREBBP (VAF)	R1602C (0.0689)	) R1602C (0.2565)	p.Phe1410LeufsTer49 (0.0058)	p.Phe1410LeufsTer49 (0.232)	wt	wt	wt	wt	wt	wt	wt	wt	wt	wt	wt	wt
ATM (VAF)	wt	wt	wt	wt	wt	wt	wt	I1581Sfs*20 (0.0071) R2227H (0.0197) p.(Ile3036Lys) (0.0134)	wt	wt	12888T (0.0053)	12888T (0.0155)	p.(Lys2700Gln) (0.009)	p.(Lys2700Gln) (0.0088)		/ V2757M ) (0.0072)
PRKDC (VAF)	wt	wt	p.(Arg489SerfsTer4) (0.0115)	p.(Arg489SerfsTer4) (0.0193)	wt	wt	wt	wt	p.(Ser2814PhefsTer5) (0.005)	wt	wt	wt	wt	wt	wt	wt
PTEN (VAF)	wt	wt	wt	wt	p.(Leu70His) (0.0054)	wt	wt	wt	wt	wt	wt	wt	N323Mfs*21 (0.0102)	N323Mfs*21 (0.0111)	wt	wt
APC (VAF)	wt	wt	wt	wt	wt	wt	p.(Ser92Thr) (0.0133)	p.(Ser92Thr) (0.0291) p.(Lys1878ArgfsTer4) (0.0051)	wt	wt	wt	wt	wt	wt	wt	wt
KRAS (VAF)	wt	wt	wt	G12D (0.0096)	wt	wt	wt	G12D (0.0657) A146T (0.0309) Q61H (0.0084) G13D (0.2197)	wt	wt	wt	wt	wt	wt	wt	wt
MAP2K1 (VAF)	wt	wt	wt	wt	wt	wt	p.(Arg108Trp) (0.1088)	p.(Arg108Trp) (0.1751)	wt	wt	wt	wt	wt	wt	wt	wt
NOTCH4 (VAF)	wt	wt	wt	wt	wt	wt	wt	wt	wt	wt	wt	wt	p.(Gly1154AlafsTer150) (0.017)	p.(Gly1154AlafsTer150) (0.0112)	wt	wt
POLD1 (VAF)	wt	wt	R126H (0.0089)	R126H (0.0288)	wt	wt	wt	wt	wt	wt	wt	wt	wt	wt	wt	wt

Abbreviations: Ct01, baseline; Ct02, time point at disease progression; VAF, variant allele frequency; wt, wild-type.

Figure 19. **Summary of genetic variants detected in colorectal cancer samples.** The table presents variant allele frequencies (VAF) for key mutations, including BRAF and PIK3CA, across different patient samples (CRC01–CRC14) and conditions (Ct01, Ct02). Data are displayed with corresponding mutation types and frequencies, highlighting interpatient variability in mutational profiles.

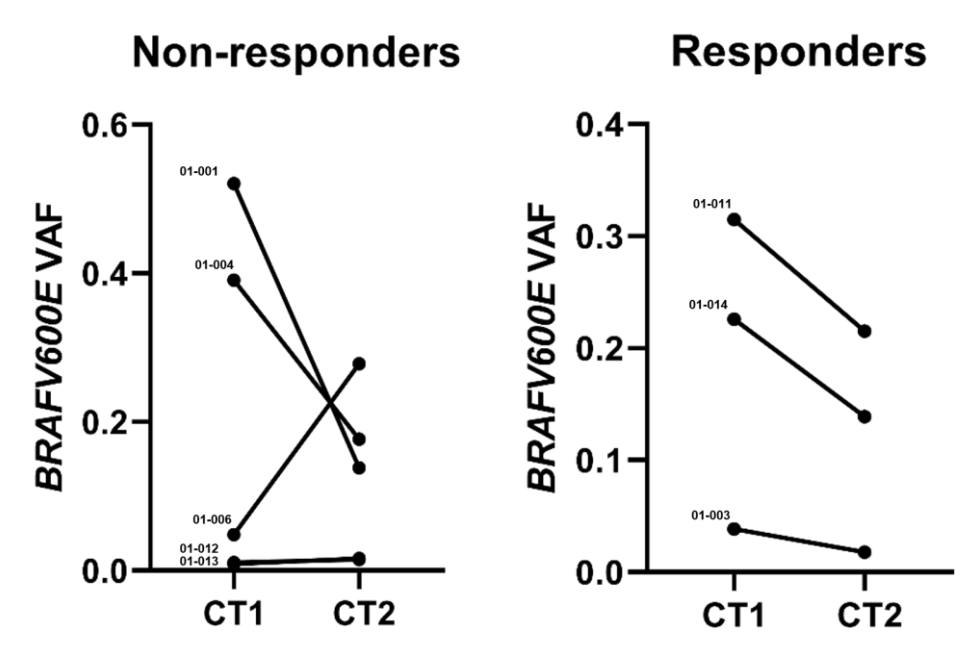


Figure 20. **CtDNA BRAFV600E status.** Variant allele frequency variation of *BRAFV600E* alteration between CT1 (baseline) and CT2 (progression disease), in responder and non-responder patients. (created with GraphPad)

### 4.4 Spatial transcriptomic preliminary analysis

The transcriptomic experiments on selected cases from our patient cohort allowed us to identify and analyze five ROIs from the tumor compartment and three ROIs from the tumor microenvironment (TME) of an NR patient, as well as four ROIs from tumor tissue and four ROIs from TME of an R patient, yielding our preliminary data (Figure 21).

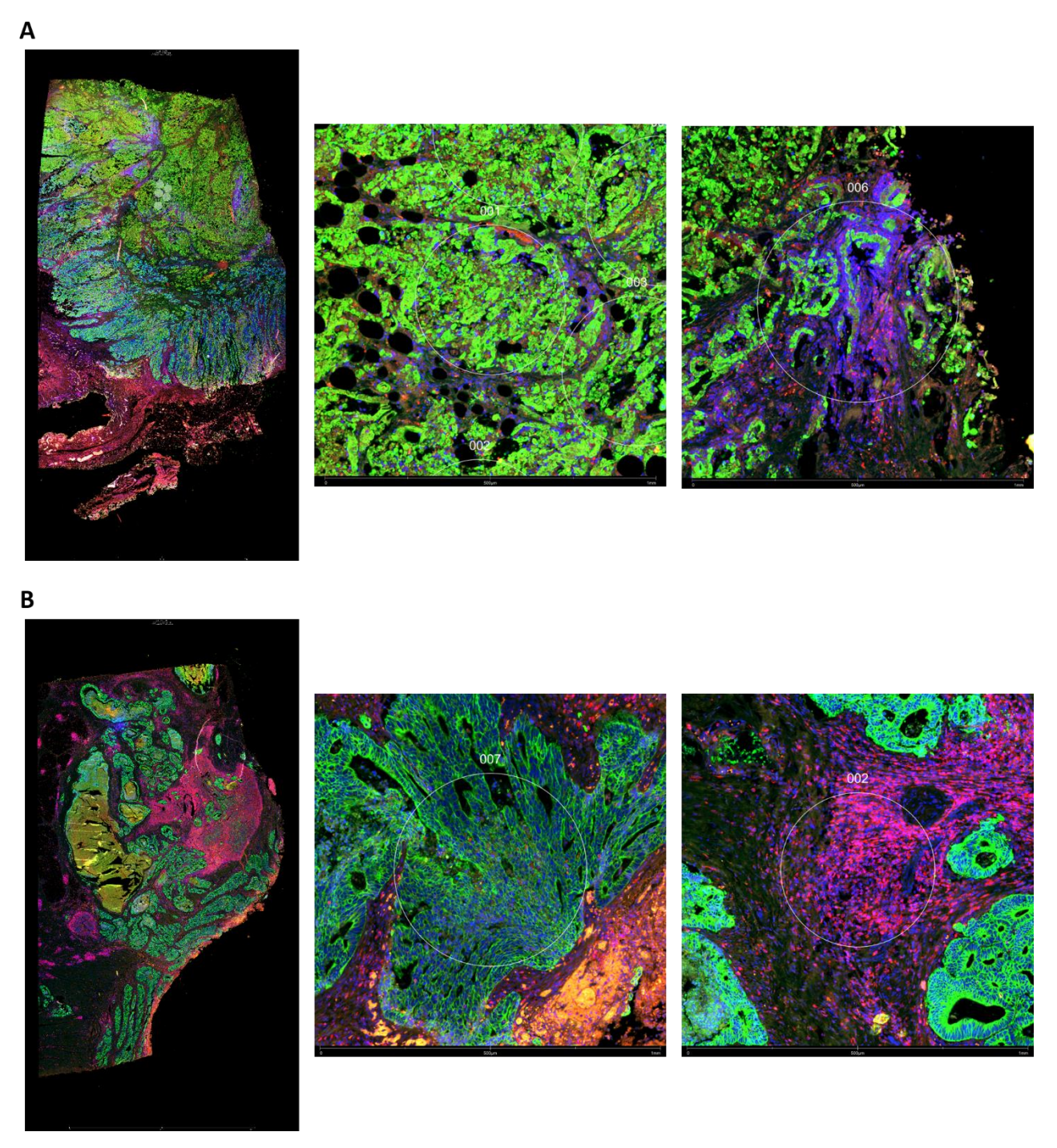


Figure 21. **Scan image of NR and R patients from GeoMx Nanostring DSP.** A) Left: Full scan of the Non-responder's tissue slide, showing an example of a ROI selected from tumor tissue and a ROI selected from the TME. B) Left: Overview of the R slide, with an image of tumor tissue staining and a ROI captured from the TME. Channels: FITC/525nm: SYTO 13: DNA: nuclei (Blue); Cy3/568nm: Alexa 532: PanCK: tumor (Green); Texas Red/615nm: Alexa 594: CD45: immune cell infiltration (Red).

A differential expression analysis was performed on the selected ROIs in the tumor tissue of R and NR patients. In the volcano plot shown in Figure 22, the gene expression profiles in the tumor areas of the NR and R groups were compared. The analysis revealed a significant upregulation of the genes

SSX1 (p= 9.25E-08) and CCL15 (p= 7.1E-08) in NR patients, whereas ACTB, EPCAM, and UBC were significantly downregulated, with p-values of 1.67E-08, 1.74E-08, and 1.67E-08, respectively. When comparing the tumor microenvironment between R and NR patients, a significant overexpression of the genes CD74 (p= 2.15E-07), HLA-DRA (p= 4.63E-08), HLA-DRB (p= 5.33E-07), COL3A1 (p= 9.09E-09), and ACTB (p= 1.4E-07) was observed in patients exhibiting a better response to treatment.

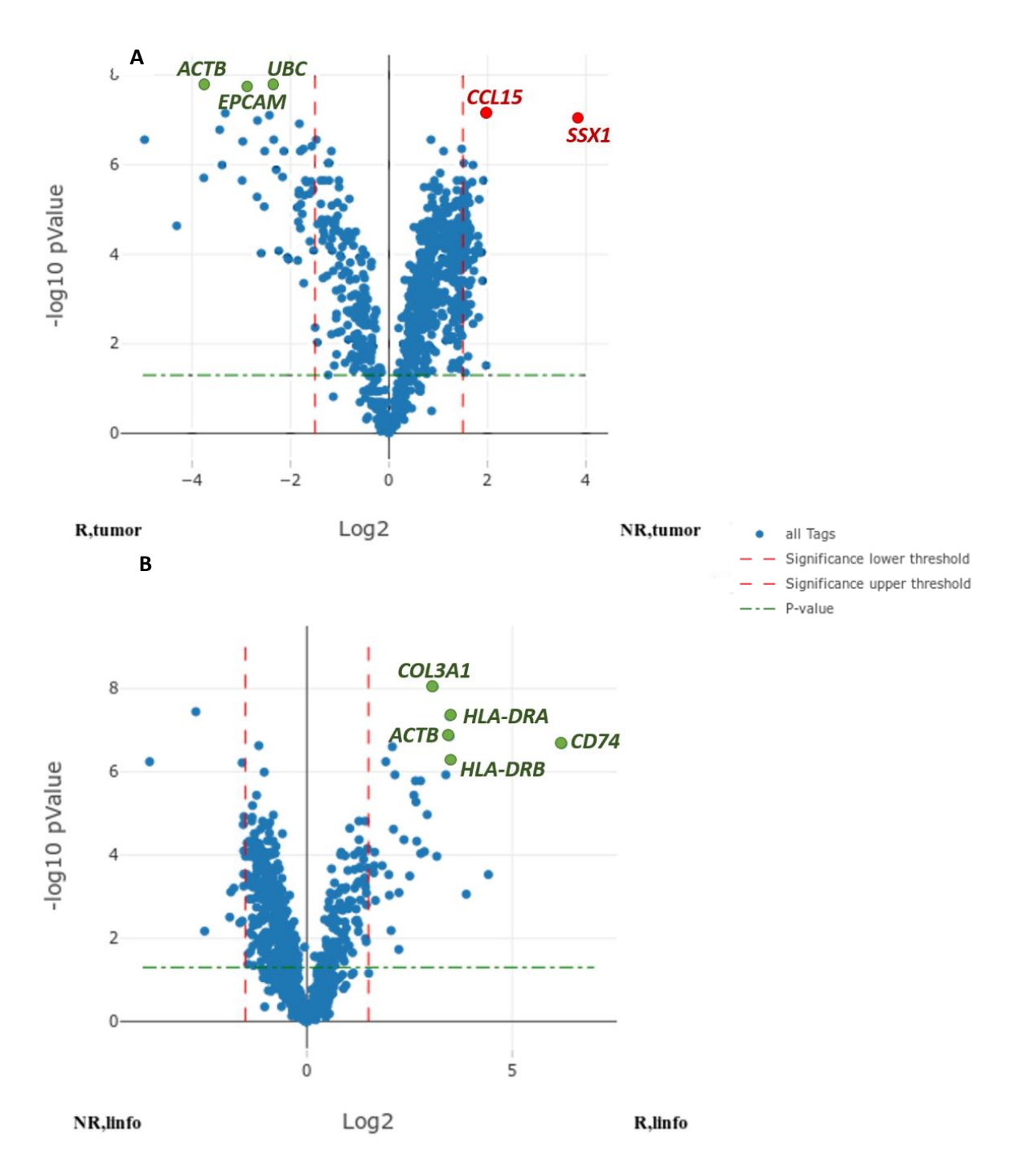


Figure 22. **Volcano plots of spatial transcriptomic analysis.** In Figure A, the expression of tumor ROIs from NR and R patients is compared. In Figure B, a differential expression analysis between TME ROIs from the same R and NR patients is shown.

Pathway analysis performed using the GeoMx Data Analysis Suite identified pathways that were differentially enriched between R and NR patients (Figure 23). In R patients, significant enrichment was observed in pathways related to cellular response to chemical agents (p=0.007), cytoprotection (p=0.008), the phagosome pathway (p=0.007), and antigen presentation processes (p=0.007). Conversely, in NR patients, enriched pathways included FGFR2 cascade activation (p=0.007), phospholipase-C cascade activation (p=0.007), GPCR receptor activation (p=0.01), chemokine receptor activation (p=0.008), and TNF receptor activation (p=0.02).

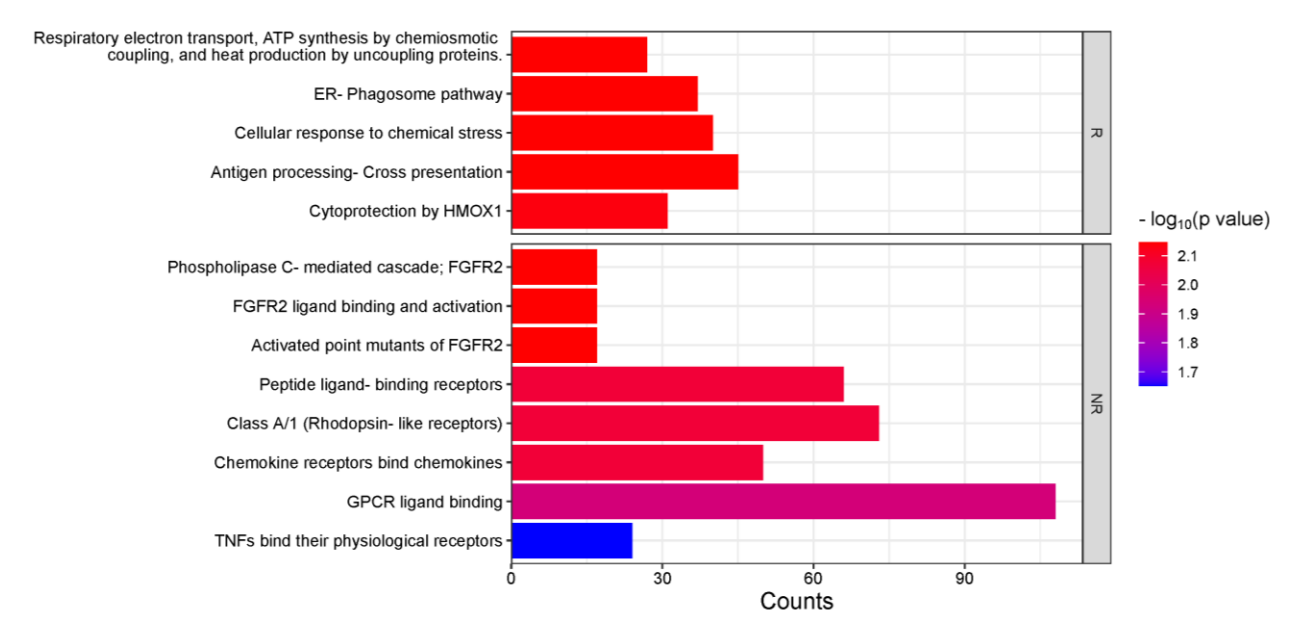


Figure 23. **Bar plot showing enriched pathways identified through transcriptomic analysis.** The upper panel highlights pathways associated with tumor-specific responses, including antigen processing and cytoprotection by HMOX1. The lower panel depicts pathways related to receptor-ligand interactions, such as GPCR ligand binding and chemokine receptor activity. The length of the bars represents the number of counts, while the color gradient indicates statistical significance (-log10(p-value)).

#### 5. DISCUSSION

The MASCARA study is an ongoing project conducted within the Biosciences Laboratory of IRST in Meldola. The aim of the project is to thoroughly investigate a subgroup of colorectal cancers with particularly poor prognosis, specifically those harboring the BRAFV600E mutation. Despite the approval of targeted therapy for use from the second line of treatment, the percentage of patients who benefit from it remains small. For this reason, the planned analyses focus on identifying both innate and acquired biomarkers of resistance in order to better stratify patients and explore new therapeutic targets that may help overcome resistance to therapy. Our data from the MASCARA study provide valuable insights into the clinical characteristics and treatment responses of patients enrolled in this cohort.

The predominance of female patients (70%) and the median age at diagnosis of 69 years align with the typical demographic profile of colorectal cancer in this population<sup>67,72</sup>. High prevalence of right-sided colon tumors (80%) reflects a characteristic feature of the disease in these patients, often associated with distinct molecular and clinical behavior compared to left-sided tumors<sup>57,73</sup>.

The universal presence of metastatic disease, with a significant proportion involving the liver (40%) and lungs (30%), underscores the aggressive nature of the disease in this cohort. Despite this, a majority of patients (76.7%) maintained an ECOG performance status of 1 at the initiation of Encorafenib plus Cetuximab, suggesting that this treatment regimen was administered to a relatively fit population.

According to literature, microsatellite instability was observed in 20% of cases, which may influence prognosis and therapeutic options, as MSI tumors are known to exhibit distinct biological characteristics and potential sensitivity to immune checkpoint inhibitors<sup>74,75</sup>.

Treatment responses, evaluated using RECIST v1.1 criteria, indicated that only 20% of patients achieved a response (complete or partial), whereas the majority (80%) were classified as non-responders, including those with stable disease or disease progression. This result aligns with data reported in the literature<sup>66</sup>. These findings underscore the challenges associated with achieving significant responses in this heavily pretreated and metastatic patient population. The results of the mutational analysis of baseline FFPE samples from this cohort provide a comprehensive overview of the molecular alterations present in colorectal cancer, with important implications for understanding treatment response. Our preliminary data confirm the role of *TP53* alterations as most frequent mutated gene in colorectal cancer tumorigenesis and its association with poor prognosis<sup>76</sup>. Similarly, *BRINP3* and *CHSY3* were frequently mutated in this cohort, consistent with the association, as reported in the literature, between mutations in these genes and poor prognosis, increased proliferation, and chemoresistance<sup>77–80</sup>. Our preliminary data also support the hypothesis that a high

percentage of MSS BRAFV600E mCRCs harbor alterations in *RNF43* and *SMAD4*. Consistent with findings by Arndt Vogel et al. and Tong, K., et al., we observed alterations in both genes in 25% of cases<sup>81,82</sup>. Moreover, mutations in these genes appear to play a role in predicting therapy response<sup>62,81–86</sup>. However, due to the limited sample size, no significant differences were observed between responders and non-responders. Overall, the mutational pattern identified in our cohort aligns with the findings reported in the literature to date<sup>71,87</sup>. Expanding the patient cohort will be necessary to validate these results. Notably, all MSI-H patients were also TMB-H, supporting the known correlation between microsatellite instability and higher tumor mutational burden<sup>88,89</sup>.

Genes already known in the literature, such as *PIK3CA* and *PTEN*, which are associated with chemoresistance or poorer prognosis not only in colorectal cancer but also in other malignancies <sup>90–94</sup>, were more frequently mutated in non-responders in our cohort.

Finally, a key finding from this analysis is the identification of novel alterations that may be associated with the lack of therapeutic response in the studied patients. In this context, *NOTCH3* mutations have been implicated in the development of chemotherapy resistance in various cancers, including colorectal cancer. *NOTCH3* is a transmembrane receptor involved in regulating cell fate, differentiation, and proliferation. In the context of chemotherapy resistance, *NOTCH3* mutations often enhance survival signaling pathways, promote epithelial-to-mesenchymal transition (EMT), and modulate the tumor microenvironment to create an immune-suppressive niche. These changes enable tumor cells to evade the cytotoxic effects of chemotherapy. The activation of NOTCH3 signaling may also affect DNA damage response mechanisms, impairing the ability of tumor cells to undergo apoptosis following chemotherapy-induced DNA damage. This allows the cancer cells to survive and proliferate despite treatment. Furthermore, *NOTCH3* mutations are associated with the upregulation of drug efflux pumps and other protective mechanisms that reduce the intracellular concentration of chemotherapy drugs, further contributing to resistance <sup>95,96</sup>.

LRP2 (Low-Density Lipoprotein Receptor-Related Protein 2) plays a significant role in the metastasis process by influencing cell adhesion, migration, and extracellular matrix remodeling. LRP2 is involved in the endocytosis of various signaling molecules and has been shown to interact with growth factors, including transforming growth factor-beta (TGF- $\beta$ ), which is crucial for epithelial-to-mesenchymal transition (EMT), a key step in metastasis. Through its regulation of these signaling pathways, LRP2 can promote the detachment of cancer cells from the primary tumor, enhance their invasive potential, and support the survival of disseminated cells in distant tissues.

Additionally, *LRP2*'s role in regulating the extracellular matrix (ECM) components facilitates tumor cell migration and invasion. By modulating the ECM, *LRP2* helps create a more permissive environment for tumor cells to invade surrounding tissues and establish metastatic lesions<sup>97</sup>.

*FBXW7* mutations contribute to chemoresistance by disrupting the degradation of key oncogenic proteins such as cyclin E, c-Myc, and Notch, which promote cell survival and proliferation. This impairs the cell's response to chemotherapy-induced DNA damage and apoptosis. Loss of *FBXW7* function enhances pro-survival pathways and DNA repair, making tumor cells more resistant to treatment <sup>98–100</sup>.

To further investigate innate resistance to targeted therapy in this tumor subtype, tissue analysis was complemented by the analysis of circulating tumor DNA (ctDNA). The objective was to evaluate the sensitivity of the method and its translatability to pre-therapy settings to enhance patient stratification. Additionally, monitoring mutations through liquid biopsy allows for the identification of alterations that arise during treatment, providing insights into mechanisms of acquired resistance.

The results presented thus far are based on a limited sample size, precluding definitive conclusions of statistical significance. However, some observations are notable. Certain mutations were detected only in tissue analysis and not through liquid biopsy, potentially due to the still-debated sensitivity of liquid biopsy techniques. Conversely, mutations identified exclusively via liquid biopsy but absent in tissue exome sequencing could be attributed to clonal hematopoiesis-associated variants (CHIP), the ability of liquid biopsy to capture tumor heterogeneity comprehensively, or differences in sequencing methodologies. Liquid biopsy employs a targeted approach (>500 genes) with higher coverage, whereas WES is broader but with lower depth<sup>101–104</sup>. Moreover, since liquid biopsy can detect mutations at very low VAF in some samples, it is crucial to validate these findings using more sensitive techniques such as digital PCR to ensure accuracy and reproducibility.

Despite these challenges, preliminary analyses revealed genes altered only in samples collected at disease progression. Consistent with findings indicating reactivation of the MAPK pathway as a primary mechanism of acquired resistance in patients treated with Encorafenib and Cetuximab, we identified several acquired genetic changes in MAPK pathway-related genes, including *RAS* mutations or amplifications and *BRAF* amplification<sup>105,106</sup>.

Another pathway associated with both innate and acquired resistance to targeted treatment is activation of the PI3K/AKT pathway. This has led to studies evaluating the administration of the triplet therapy Encorafenib, Cetuximab, and Alpelisib<sup>105,107,108</sup>. In this context, we identified *PIK3CA* mutations in patient blood samples at disease progression.

Interestingly, a patient harboring a *MAP2K1* mutation was found to be non-responsive to the combination of encorafenib and cetuximab, suggesting that most of these mutations are primarily RAF-dependent and therefore sensitive to MEK inhibition<sup>71</sup>. Furthermore, a significant proportion of NR exhibited *SMAD4* mutations, even at disease progression. Our findings corroborate that the loss of SMAD4 function may disrupt feedback mechanisms within the TGF-β pathway, indirectly

sustaining MAPK activity or activating alternative survival pathways. This disruption contributes to resistance against MAPK pathway-targeting therapies<sup>62</sup>.

Another result of interest is the identification of *PRKDC* mutations in responsive patients. Emerging evidence suggests that *PRKDC* (Protein Kinase, DNA-Activated, Catalytic Subunit), involved in DNA damage repair through the non-homologous end-joining (NHEJ) pathway, may influence the tumor microenvironment and affect treatment responsiveness. For instance, *PRKDC*-deficient cells may exhibit increased sensitivity to DNA-damaging agents, such as radiation or platinum-based chemotherapy, due to impaired DNA repair capacity<sup>109,110</sup>.

The variation in the variant allele frequency (VAF) of *BRAFV600*E between baseline and PD during treatment with Encorafenib plus Cetuximab provides valuable insights into therapeutic response and resistance mechanisms in CRC. At baseline, a high VAF typically reflects a clonal *BRAFV600E* mutation, indicating tumor dependency on the MAPK pathway and a higher likelihood of an initial response to targeted therapy. However, at PD, changes in *BRAFV600E* VAF, such as a decrease, may suggest clonal evolution or the emergence of resistance driven by alternative pathways or subclonal populations. Conversely, a stable or increased VAF at PD indicates continued reliance on BRAF signaling despite therapy. These dynamics highlight the significance of intratumoral heterogeneity and the selection of resistant clones during treatment 111.

Consistent with this hypothesis, in our cohort, all patients who achieved a CR or PR exhibited a reduction in *BRAFV600E* VAF until PD.

The TME plays a pivotal role in influencing how drugs interact with tumor cells and immune components, often contributing to resistance. Factors such as immune cells, stromal cells, and extracellular matrix components within the TME can affect the efficacy of targeted therapy, potentially limiting their therapeutic potential. Many studies have investigated the role of the TME in MSS and MSI-H *BRAF V600E*-mutant CRC to identify more effective therapeutic combinations<sup>74</sup>. Within this context, our MASCARA project aims to conduct an in-depth investigation of these aspects to advance the understanding of resistance mechanisms and improve therapeutic strategies. The differential gene expression analysis conducted on selected regions of interest in tumor tissues from R and NR patients has provided insightful findings regarding the molecular differences associated with treatment response in colorectal cancer.

In the NR group, the upregulation of SSXI (p = 9.25E-08) and CCL15 (p = 7.1E-08) suggests a potential role in tumor progression and resistance mechanisms. SSXI, a member of the synovial sarcoma family, has been associated with various cancers and may contribute to immune evasion or cellular proliferation<sup>112–115</sup>. CCL15, a chemokine, is involved in immune cell recruitment and could indicate an altered immune landscape in NR tumors, which may facilitate the survival and spread of

cancer cells. The upregulation of these genes could potentially reflect an environment that promotes tumor growth and resistance to treatment, highlighting their relevance as biomarkers of poor prognosis<sup>116,117</sup>.

On the other hand, the downregulation of *ACTB*, *EPCAM*, and *UBC* in NR patients (p-values of 1.67E-08, 1.74E-08, and 1.67E-08, respectively) may suggest the loss of key cellular functions critical for tumor suppression or cellular adhesion. *ACTB* is a cytoskeletal protein involved in cell motility, and its downregulation might indicate disruption of cell structure and potentially contribute to invasive behavior in non-responder tumors. Similarly, *EPCAM*, a cell adhesion molecule, is important for epithelial cell integrity and its downregulation could be associated with epithelial-to-mesenchymal transition (EMT), a process linked to metastasis and resistance <sup>118,119</sup>. *UBC*, a gene encoding a component of the ubiquitin-proteasome system, is crucial for protein degradation, and its reduced expression may impair the ability of cancer cells to regulate cell cycle and survival, contributing to resistance to therapy<sup>120</sup>.

In contrast, the R group showed a distinct pattern of gene overexpression, particularly in immune-related genes and extracellular matrix components. The overexpression of CD74 (p = 2.15E-07), HLA-DRA (p = 4.63E-08), and HLA-DRB (p = 5.33E-07) suggests an active involvement of the immune system in the tumor response. These genes are key components of the major histocompatibility complex (MHC) class II molecules, which play a critical role in antigen presentation and the activation of T-helper cells. Their upregulation could reflect an enhanced immune response in R patients, which may facilitate the recognition and elimination of tumor cells (10.3389/fimmu.2019.01426, 10.1038/onc.2016.161). Additionally, COL3A1 (p = 9.09E-09), an extracellular matrix protein involved in tissue remodeling, was significantly overexpressed in responder patients, suggesting that TME in these patients may be more conducive to an immune-active and anti-tumor response<sup>121</sup>.

Furthermore, the significant overexpression of ACTB (p = 1.4E-07) in the responder group, in contrast to its downregulation in NR patients, may indicate that maintaining cytoskeletal integrity is critical for effective tumor response to therapy. The preservation of ACTB expression could promote cellular adhesion and motility, facilitating the proper function of immune cells within TME.

These findings suggest that the gene expression profiles in both the tumor tissue and the tumor microenvironment differ significantly between responder and non-responder patients. In particular, the immune-related gene upregulation in responders indicates that a functional immune system might play a pivotal role in treatment efficacy, possibly through the enhancement of immune surveillance and tumor cell recognition. Conversely, the upregulation of immune evasion and tumor-promoting genes in non-responders points to a more immune-suppressive and resistant TME<sup>122</sup>.

However, it is important to note that these results have limitations in terms of statistical significance, as they are based on preliminary data obtained from only two patients. Thus, the findings should be interpreted with caution, and further validation in a larger cohort is required to confirm the robustness and clinical relevance of these observations.

The differential expression of genes such as *SSX1*, *CCL15*, *HLA-DRA*, and *CD74* could serve as potential biomarkers for predicting treatment response in colorectal cancer. These genes may be used to stratify patients into different risk groups, allowing for more personalized treatment regimens. The downregulation of *ACTB*, *EPCAM*, and *UBC* in non-responders suggests that targeting the molecular mechanisms underlying these changes might help to sensitize tumors to therapy. For example, strategies aimed at restoring the function of the ubiquitin-proteasome system or targeting *EPCAM* could potentially overcome resistance mechanisms in these patients.

Moreover, therapies that enhance immune activation, such as immune checkpoint inhibitors or cancer vaccines, could be particularly beneficial for patients showing high expression of immune-related genes like *CD74* and *HLA-DR*. Conversely, for patients with tumors characterized by immune evasion, such as those exhibiting high levels of *SSX1* and *CCL15*, combination therapies targeting both the tumor cells and the immune microenvironment may be necessary <sup>123–126</sup>.

Finally, the pathway analysis performed using the GeoMx Data Analysis Suite revealed distinct differences in pathway enrichment between R and NR patients. In R patients, significant enrichment was observed in pathways associated with immune activation and cellular protection, including the cellular response to chemical agents (p = 0.007), cytoprotection (p = 0.008), phagosome pathway (p = 0.007), and antigen presentation processes (p = 0.007). These pathways suggest that responders may have an active immune system capable of effectively recognizing and responding to tumor cells. The enrichment in antigen presentation and phagosome pathways indicates enhanced immune surveillance, potentially facilitating the recognition and elimination of cancer cells. Additionally, pathways related to cytoprotection may reflect the tumor's ability to protect healthy cells from the effects of therapy, promoting therapeutic efficacy<sup>127–129</sup>.

Conversely, in NR patients, pathways linked to cellular survival and immune evasion were enriched, including FGFR2 cascade activation (p = 0.007), phospholipase-C cascade activation (p = 0.007), GPCR receptor activation (p = 0.01), chemokine receptor activation (p = 0.008), and TNF receptor activation (p = 0.02). These pathways are associated with tumor growth, inflammation, and immune suppression.

The PLC pathway's interaction with chemokine receptor and GPCR activation further supports immune suppression, reinforcing the tumor's ability to evade therapy<sup>130–133</sup>. The activation of FGFR2 and GPCR signaling, in particular, suggests that NR tumors may rely on pro-survival signaling

pathways to evade treatment, while chemokine receptor activation and TNF receptor activation may contribute to an immune-suppressive microenvironment, preventing effective immune responses against the tumor<sup>134–136</sup>.

The MASCARA study reveals significant molecular differences between responders and non-responders in *BRAFV600E*-mutant colorectal cancer. Key biomarkers and pathways were identified that could guide patient stratification and treatment strategies. Genomic analysis showed frequent mutations in *TP53*, *BRINP3*, *CHSY3*, and *SMAD4*, linked to poor prognosis and chemoresistance, with *RNF43* and *SMAD4* alterations observed in 25% of cases, potentially predicting therapy response. Non-responders had more mutations in *PIK3CA*, *PTEN*, and *PRKDC*, along with an immune-suppressive tumor microenvironment characterized by the upregulation of *SSX1* and *CCL15* and the downregulation of *ACTB* and *EPCAM*. In contrast, responders exhibited increased expression of immune-related genes like *CD74* and *HLA-DRA*, with immune activation and cellular protection pathways enriched in their tumors. These findings provide valuable insights into the mechanisms of both innate and acquired resistance, supporting the need for further investigation and the development of personalized therapeutic approaches.

#### 6. FUTURE PERSPECTIVE

The results obtained in this study have limitations due to the small sample size and the lack of statistical analysis. Further investigation involving larger cohorts and comprehensive statistical evaluations is essential to confirm the true significance and generalizability of these results.

Future efforts will focus on completing the patient enrollment to reach the target number required for the project. This will allow for a more robust correlation of clinical data with progression-free survival (PFS) and overall survival (OS) as well as radiological imaging. Additionally, further molecular analyses will be conducted to deepen our understanding of the tumor biology. Special attention will be given to investigating the role of the immune system, both at the tumor site and peripherally, in determining the response to therapy. These expanded analyses will provide more comprehensive insights into the mechanisms driving treatment efficacy and resistance, ultimately contributing to more personalized therapeutic approaches.

#### 7. REFERENCES

- 1. Bray, F. *et al.* Global cancer statistics 2022: GLOBOCAN estimates of incidence and mortality worldwide for 36 cancers in 185 countries. *CA. Cancer J. Clin.* **74**, 229–263 (2024).
- 2. Eng, C. et al. Colorectal cancer. Lancet 404, 294–310 (2024).
- 3. Roshandel, G., Ghasemi-Kebria, F. & Malekzadeh, R. Colorectal Cancer: Epidemiology, Risk Factors, and Prevention. *Cancers (Basel)*. **16**, 1530 (2024).
- 4. McNabb, S. *et al.* Meta-analysis of 16 studies of the association of alcohol with colorectal cancer. *Int. J. cancer* **146**, 861–873 (2020).
- 5. Cai, S., Li, Y., Ding, Y., Chen, K. & Jin, M. Alcohol drinking and the risk of colorectal cancer death. *Eur. J. Cancer Prev.* **23**, 532–539 (2014).
- 6. Botteri, E. *et al.* Smoking and Colorectal Cancer Risk, Overall and by Molecular Subtypes: A Meta-Analysis. *Am. J. Gastroenterol.* **115**, 1940–1949 (2020).
- 7. Lauby-Secretan, B. *et al.* Body Fatness and Cancer Viewpoint of the IARC Working Group. *N. Engl. J. Med.* **375**, 794–798 (2016).
- 8. Soltani, G. *et al.* Obesity, diabetes and the risk of colorectal adenoma and cancer. *BMC Endocr. Disord.* **19**, 113 (2019).
- 9. Morrow, L. & Greenwald, B. Healthy Food Choices, Physical Activity, and Screening Reduce the Risk of Colorectal Cancer. *Gastroenterol. Nurs.* **45**, 113–119 (2022).
- 10. Domingo, J. L. & Nadal, M. Carcinogenicity of consumption of red meat and processed meat: A review of scientific news since the IARC decision. *Food Chem. Toxicol.* **105**, 256–261 (2017).
- 11. Pearlman, R. *et al.* Prevalence and Spectrum of Germline Cancer Susceptibility Gene Mutations Among Patients With Early-Onset Colorectal Cancer. *JAMA Oncol.* **3**, 464 (2017).
- 12. Taylor, D. P. *et al.* How well does family history predict who will get colorectal cancer? Implications for cancer screening and counseling. *Genet. Med.* **13**, 385–391 (2011).
- 13. Olén, O. *et al.* Colorectal cancer in ulcerative colitis: a Scandinavian population-based cohort study. *Lancet* **395**, 123–131 (2020).
- 14. Yamada, A. *et al.* Risk of gastrointestinal cancers in patients with cystic fibrosis: a systematic review and meta-analysis. *Lancet Oncol.* **19**, 758–767 (2018).
- 15. Maida, M. *et al.* Screening and Surveillance of Colorectal Cancer: A Review of the Literature. *Cancers (Basel).* **16**, 2746 (2024).
- 16. Imperiale, T. F. *et al.* Multitarget Stool DNA Testing for Colorectal-Cancer Screening. *N. Engl. J. Med.* **370**, 1287–1297 (2014).
- 17. Lopes, S. R. et al. Colorectal cancer screening: A review of current knowledge and progress

- in research. World J. Gastrointest. Oncol. 16, 1119–1133 (2024).
- 18. Shaukat, A. & Levin, T. R. Current and future colorectal cancer screening strategies. *Nat. Rev. Gastroenterol. Hepatol.* **19**, 521–531 (2022).
- 19. Song, L.-L. & Li, Y.-M. Current noninvasive tests for colorectal cancer screening: An overview of colorectal cancer screening tests. *World J. Gastrointest. Oncol.* **8**, 793 (2016).
- 20. Helsingen, L. M. & Kalager, M. Colorectal Cancer Screening Approach, Evidence, and Future Directions. *NEJM Evid.* **1**, (2022).
- 21. Wolf, A. M. D. *et al.* Colorectal cancer screening for average-risk adults: 2018 guideline update from the American Cancer Society. *CA. Cancer J. Clin.* **68**, 250–281 (2018).
- 22. Qaseem, A., Crandall, C. J., Mustafa, R. A., Hicks, L. A. & Wilt, T. J. Screening for Colorectal Cancer in Asymptomatic Average-Risk Adults: A Guidance Statement From the American College of Physicians. *Ann. Intern. Med.* **171**, 643–654 (2019).
- 23. Rex, D. K. *et al.* American College of Gastroenterology Guidelines for Colorectal Cancer Screening 2008. *Am. J. Gastroenterol.* **104**, 739–750 (2009).
- 24. Vasen, H. F. A. *et al.* Guidelines for the clinical management of Lynch syndrome (hereditary non-polyposis cancer). *J. Med. Genet.* **44**, 353–362 (2007).
- 25. Continuing Medical Education: June 2015. Am. J. Gastroenterol. 110, 835 (2015).
- 26. Benchimol, E. I. *et al.* Rural and Urban Residence During Early Life is Associated with Risk of Inflammatory Bowel Disease: A Population-Based Inception and Birth Cohort Study. *Am. J. Gastroenterol.* **112**, 1412–1422 (2017).
- 27. Ahlquist, D. A. Molecular Detection of Colorectal Neoplasia. *Gastroenterology* **138**, 2127–2139 (2010).
- 28. Dekker, E., Tanis, P. J., Vleugels, J. L. A., Kasi, P. M. & Wallace, M. B. Colorectal cancer. *Lancet* **394**, 1467–1480 (2019).
- 29. Benson, A. B. *et al.* Colon Cancer, Version 3.2024, NCCN Clinical Practice Guidelines in Oncology. *J. Natl. Compr. Cancer Netw.* **22**, (2024).
- 30. Grady, W. M. & Markowitz, S. D. The Molecular Pathogenesis of Colorectal Cancer and Its Potential Application to Colorectal Cancer Screening. *Dig. Dis. Sci.* **60**, 762–772 (2015).
- 31. Al-Joufi, F. *et al.* Molecular Pathogenesis of Colorectal Cancer with an Emphasis on Recent Advances in Biomarkers, as Well as Nanotechnology-Based Diagnostic and Therapeutic Approaches. *Nanomaterials* **12**, 169 (2022).
- 32. Arnold, C. N., Goel, A., Blum, H. E. & Richard Boland, C. Molecular pathogenesis of colorectal cancer. *Cancer* **104**, 2035–2047 (2005).
- 33. Guinney, J. et al. The consensus molecular subtypes of colorectal cancer. Nat. Med. 21, 1350–

- 6 (2015).
- 34. Mouillet-Richard, S. *et al.* Clinical Challenges of Consensus Molecular Subtype CMS4 Colon Cancer in the Era of Precision Medicine. *Clin. Cancer Res.* **30**, 2351–2358 (2024).
- 35. 'AJCC Cancer Staging Manual,' 8th Edition. https://cancerstaging.org.
- 36. Siegel, R. L., Miller, K. D. & Jemal, A. Cancer statistics, 2020. *CA. Cancer J. Clin.* **70**, 7–30 (2020).
- 37. Edge, S. B. & Compton, C. C. The American Joint Committee on Cancer: the 7th Edition of the AJCC Cancer Staging Manual and the Future of TNM. *Ann. Surg. Oncol.* **17**, 1471–1474 (2010).
- 38. Goere, D. *et al.* Results of a randomized phase 3 study evaluating the potential benefit of a second-look surgery plus HIPEC in patients at high risk of developing colorectal peritoneal metastases (PROPHYLOCHIP- NTC01226394). *J. Clin. Oncol.* **36**, 3531–3531 (2018).
- 39. Le, D. T. *et al.* Mismatch repair deficiency predicts response of solid tumors to PD-1 blockade. *Science* (80-. ). **357**, 409–413 (2017).
- 40. Amado, R. G. *et al.* Wild-Type KRAS Is Required for Panitumumab Efficacy in Patients With Metastatic Colorectal Cancer. *J. Clin. Oncol.* **26**, 1626–1634 (2008).
- 41. Argilés, G. *et al.* Localised colon cancer: ESMO Clinical Practice Guidelines for diagnosis, treatment and follow-up. *Ann. Oncol.* **31**, 1291–1305 (2020).
- 42. Cervantes, A. *et al.* Metastatic colorectal cancer: ESMO Clinical Practice Guideline for diagnosis, treatment and follow-up. *Ann. Oncol.* **34**, 10–32 (2023).
- 43. Mazouji, O., Ouhajjou, A., Incitti, R. & Mansour, H. Updates on Clinical Use of Liquid Biopsy in Colorectal Cancer Screening, Diagnosis, Follow-Up, and Treatment Guidance. *Front. Cell Dev. Biol.* **9**, (2021).
- 44. Vacante, M., Ciuni, R., Basile, F. & Biondi, A. The Liquid Biopsy in the Management of Colorectal Cancer: An Overview. *Biomedicines* **8**, 308 (2020).
- 45. Torresan, S. *et al.* Liquid biopsy in colorectal cancer: Onward and upward. *Crit. Rev. Oncol. Hematol.* **194**, 104242 (2024).
- 46. Tao, X.-Y., Li, Q.-Q. & Zeng, Y. Clinical application of liquid biopsy in colorectal cancer: detection, prediction, and treatment monitoring. *Mol. Cancer* **23**, 145 (2024).
- 47. Wang, Z. *et al.* Liquid biopsy for monitoring minimal residual disease in colorectal cancer: A promising approach with clinical implications. *Clin. Surg. Oncol.* **3**, 100056 (2024).
- 48. Mauri, G. *et al.* Liquid biopsies to monitor and direct cancer treatment in colorectal cancer. *Br. J. Cancer* **127**, 394–407 (2022).
- 49. Bond, C. E. & Whitehall, V. L. J. How the BRAF V600E Mutation Defines a Distinct

- Subgroup of Colorectal Cancer: Molecular and Clinical Implications. *Gastroenterol. Res. Pract.* **2018**, 1–14 (2018).
- 50. Piercey, O. *et al.* BRAF-Mutant Metastatic Colorectal Cancer: Current Evidence, Future Directions, and Research Priorities. *Clin. Colorectal Cancer* **23**, 215–229 (2024).
- 51. Poulikakos, P. I., Sullivan, R. J. & Yaeger, R. Molecular Pathways and Mechanisms of BRAF in Cancer Therapy. *Clin. Cancer Res.* **28**, 4618–4628 (2022).
- 52. 1000 Genomes Project Consortium *et al.* A global reference for human genetic variation. *Nature* **526**, 68–74 (2015).
- 53. Chen, D. *et al.* BRAFV600E Mutation and Its Association with Clinicopathological Features of Colorectal Cancer: A Systematic Review and Meta-Analysis. *PLoS One* **9**, e90607 (2014).
- 54. Sholl, L. M. A narrative review of BRAF alterations in human tumors: diagnostic and predictive implications. *Precis. Cancer Med.* **3**, 26–26 (2020).
- 55. Scott, B. Updates in BRAF V600E-Mutated Metastatic Colorectal Cancer. *EMJ Oncol.* 2–12 (2024) doi:10.33590/emjoncol/JDXK9403.
- 56. Jones, J. C. *et al.* Non-V600 BRAF Mutations Define a Clinically Distinct Molecular Subtype of Metastatic Colorectal Cancer. *J. Clin. Oncol.* **35**, 2624–2630 (2017).
- 57. Fanelli, G. N. *et al.* The heterogeneous clinical and pathological landscapes of metastatic Brafmutated colorectal cancer. *Cancer Cell Int.* **20**, 30 (2020).
- 58. Clarke, C. N. & Kopetz, E. S. BRAF mutant colorectal cancer as a distinct subset of colorectal cancer: clinical characteristics, clinical behavior, and response to targeted therapies. *J. Gastrointest. Oncol.* **6**, 660–7 (2015).
- 59. Barras, D. *et al.* BRAF V600E Mutant Colorectal Cancer Subtypes Based on Gene Expression. *Clin. Cancer Res.* **23**, 104–115 (2017).
- 60. Schirripa, M. *et al.* Class 1, 2, and 3 BRAF-Mutated Metastatic Colorectal Cancer: A Detailed Clinical, Pathologic, and Molecular Characterization. *Clin. Cancer Res.* **25**, 3954–3961 (2019).
- 61. Overman, M. J. *et al.* Nivolumab in patients with metastatic DNA mismatch repair-deficient or microsatellite instability-high colorectal cancer (CheckMate 142): an open-label, multicentre, phase 2 study. *Lancet. Oncol.* **18**, 1182–1191 (2017).
- 62. Ye, L.-F. *et al.* Monitoring tumour resistance to the BRAF inhibitor combination regimen in colorectal cancer patients via circulating tumour DNA. *Drug Resist. Updat.* **65**, 100883 (2022).
- 63. Jang, M. H. *et al.* BRAF -Mutated Colorectal Cancer Exhibits Distinct Clinicopathological Features from Wild-Type BRAF -Expressing Cancer Independent of the Microsatellite Instability Status. *J. Korean Med. Sci.* **32**, 38 (2017).

- 64. Kopetz, S. *et al.* Encorafenib, Binimetinib, and Cetuximab in BRAF V600E–Mutated Colorectal Cancer. *N. Engl. J. Med.* **381**, 1632–1643 (2019).
- 65. Kopetz, S. *et al.* Randomized Trial of Irinotecan and Cetuximab With or Without Vemurafenib in BRAF-Mutant Metastatic Colorectal Cancer (SWOG S1406). *J. Clin. Oncol.* **39**, 285–294 (2021).
- 66. Tabernero, J. *et al.* Encorafenib Plus Cetuximab as a New Standard of Care for Previously Treated BRAF V600E-Mutant Metastatic Colorectal Cancer: Updated Survival Results and Subgroup Analyses from the BEACON Study. *J. Clin. Oncol.* **39**, 273–284 (2021).
- 67. Martinelli, E. *et al.* Real-world first-line treatment of patients with BRAFV600E-mutant metastatic colorectal cancer: the CAPSTAN CRC study. *ESMO Open* **7**, 100603 (2022).
- 68. Grothey, A., Fakih, M. & Tabernero, J. Management of BRAF-mutant metastatic colorectal cancer: a review of treatment options and evidence-based guidelines. *Ann. Oncol.* **32**, 959–967 (2021).
- 69. Motta Guerrero, R. *et al.* Targeting BRAF V600E in metastatic colorectal cancer: where are we today? *Ecancermedicalscience* **16**, (2022).
- 70. Germani, M. M. *et al.* Treatment of patients with BRAF-mutated metastatic colorectal cancer after progression to encorafenib and cetuximab: data from a real-world nationwide dataset. *ESMO Open* **9**, 102996 (2024).
- 71. Kopetz, S. *et al.* Molecular profiling of BRAF-V600E-mutant metastatic colorectal cancer in the phase 3 BEACON CRC trial. *Nat. Med.* **30**, 3261–3271 (2024).
- 72. Fanelli, G. N. *et al.* The heterogeneous clinical and pathological landscapes of metastatic Brafmutated colorectal cancer. *Cancer Cell Int.* **20**, 30 (2020).
- 73. Ueda, K. *et al.* BRAF V600E mutations in right-side colon cancer: Heterogeneity detected by liquid biopsy. *Eur. J. Surg. Oncol.* **48**, 1375–1383 (2022).
- 74. Tian, J. *et al.* Combined PD-1, BRAF and MEK inhibition in BRAFV600E colorectal cancer: a phase 2 trial. *Nat. Med.* **29**, 458–466 (2023).
- 75. Comprehensive molecular characterization of human colon and rectal cancer. *Nature* **487**, 330–337 (2012).
- 76. Chen, X. *et al.* Mutant p53 in cancer: from molecular mechanism to therapeutic modulation. *Cell Death Dis.* **13**, 974 (2022).
- 77. Zeng, W. *et al.* Overexpression of BRINP3 Predicts Poor Prognosis and Promotes Cancer Cell Proliferation and Migration via MAP4 in Osteosarcoma. *Dis. Markers* **2022**, 1–10 (2022).
- 78. Wang, H. *et al.* The prognostic implications and tumor-promoting functions of CHSY3 in gastric cancer. *Front. Immunol.* **15**, (2024).

- 79. Li, X. *et al.* CHSY3 can be a Poor Prognostic Biomarker and Mediates Immune Evasion in Stomach Adenocarcinoma. *Front. Genet.* **13**, (2022).
- 80. Huang, X. *et al.* CHSY3 promotes proliferation and migration in gastric cancer and is associated with immune infiltration. *J. Transl. Med.* **21**, 474 (2023).
- 81. Vogel, A. *et al.* Association of RNF43 Genetic Alterations With BRAF V600E and MSI high in Colorectal Cancer. *JCO Precis. Oncol.* (2024) doi:10.1200/PO.23.00411.
- 82. Tong, K. *et al.* SMAD4 is critical in suppression of BRAF-V600E serrated tumorigenesis. *Oncogene* **40**, 6034–6048 (2021).
- 83. Buchanan, D. D. *et al.* Lack of evidence for germline RNF43 mutations in patients with serrated polyposis syndrome from a large multinational study. *Gut* **66**, 1170–1172 (2017).
- 84. Yan, H. H. N. *et al.* RNF43 germline and somatic mutation in serrated neoplasia pathway and its association with BRAF mutation. *Gut* **66**, 1645–1656 (2017).
- 85. Quintanilha, J. C. F., Graf, R. P. & Oxnard, G. R. BRAF V600E and RNF43 Co-mutations Predict Patient Outcomes with Targeted Therapies in Real-World Cases of Colorectal Cancer. *Oncologist* **28**, e171–e174 (2023).
- 86. Elez, E. *et al.* RNF43 mutations predict response to anti-BRAF/EGFR combinatory therapies in BRAFV600E metastatic colorectal cancer. *Nat. Med.* **28**, 2162–2170 (2022).
- 87. Ji, J., Sandhu, J., Wang, C. & Fakih, M. Metastatic pattern is a prognostic factor in BRAF mutant colorectal cancer. *Cancer Treat. Res. Commun.* **35**, 100714 (2023).
- 88. Schrock, A. B. *et al.* Tumor mutational burden is predictive of response to immune checkpoint inhibitors in MSI-high metastatic colorectal cancer. *Ann. Oncol.* **30**, 1096–1103 (2019).
- 89. Huang, X. *et al.* Characterization of tumor mutation burden (TMB) and microsatellite instability (MSI) interplay for gastroesophageal adenocarcinoma (GA) and colorectal carcinoma (CRC). *J. Clin. Oncol.* **36**, 22–22 (2018).
- 90. Samuels, Y. & Waldman, T. Oncogenic mutations of PIK3CA in human cancers. *Curr. Top. Microbiol. Immunol.* **347**, 21–41 (2010).
- 91. Mao, C., Yang, Z. Y., Hu, X. F., Chen, Q. & Tang, J. L. PIK3CA exon 20 mutations as a potential biomarker for resistance to anti-EGFR monoclonal antibodies in KRAS wild-type metastatic colorectal cancer: a systematic review and meta-analysis. *Ann. Oncol.* 23, 1518–1525 (2012).
- 92. Song, M. S., Salmena, L. & Pandolfi, P. P. The functions and regulation of the PTEN tumour suppressor. *Nat. Rev. Mol. Cell Biol.* **13**, 283–296 (2012).
- 93. Yuan, T. L. & Cantley, L. C. PI3K pathway alterations in cancer: variations on a theme. *Oncogene* **27**, 5497–5510 (2008).

- 94. Meric-Bernstam, F. *et al.* PIK3CA/PTEN Mutations and Akt Activation As Markers of Sensitivity to Allosteric mTOR Inhibitors. *Clin. Cancer Res.* **18**, 1777–1789 (2012).
- 95. George, D. C., Bertrand, F. E. & Sigounas, G. Notch-3 affects chemoresistance in colorectal cancer via DNA base excision repair enzymes. *Adv. Biol. Regul.* **91**, 101013 (2024).
- 96. Shaik, J. P. *et al.* Frequent Activation of Notch Signaling Pathway in Colorectal Cancers and Its Implication in Patient Survival Outcome. *J. Oncol.* **2020**, 1–8 (2020).
- 97. Zheng, X. *et al.* LDL receptor related protein 2 to promote colorectal cancer metastasis via enhancing GSK3β/β-catenin signaling. *J. Clin. Oncol.* **39**, e15507–e15507 (2021).
- 98. Boretto, M. *et al.* Epidermal growth factor receptor (EGFR) is a target of the tumor-suppressor E3 ligase FBXW7. *Proc. Natl. Acad. Sci.* **121**, (2024).
- 99. Tong, J., Tan, S., Zou, F., Yu, J. & Zhang, L. FBW7 mutations mediate resistance of colorectal cancer to targeted therapies by blocking Mcl-1 degradation. *Oncogene* **36**, 787–796 (2017).
- 100. Lorenzi, F., Babaei-Jadidi, R., Sheard, J., Spencer-Dene, B. & Nateri, A. S. Fbxw7-associated drug resistance is reversed by induction of terminal differentiation in murine intestinal organoid culture. *Mol. Ther. Methods Clin. Dev.* **3**, 16024 (2016).
- 101. Boukovala, M., Westphalen, C. B. & Probst, V. Liquid biopsy into the clinics: Current evidence and future perspectives. *J. Liq. Biopsy* **4**, 100146 (2024).
- 102. Adhit, K. K., Wanjari, A., Menon, S. & K, S. Liquid Biopsy: An Evolving Paradigm for Non-invasive Disease Diagnosis and Monitoring in Medicine. *Cureus* (2023) doi:10.7759/cureus.50176.
- 103. Ho, H.-Y., Chung, K.-S. (Kasey), Kan, C.-M. & Wong, S.-C. (Cesar). Liquid Biopsy in the Clinical Management of Cancers. *Int. J. Mol. Sci.* **25**, 8594 (2024).
- 104. Parikh, A. R. *et al.* Liquid versus tissue biopsy for detecting acquired resistance and tumor heterogeneity in gastrointestinal cancers. *Nat. Med.* **25**, 1415–1421 (2019).
- 105. Ros, J. *et al.* Encorafenib plus cetuximab for the treatment of BRAF-V600E -mutated metastatic colorectal cancer. *Therap. Adv. Gastroenterol.* **15**, (2022).
- 106. Xu, T. *et al.* Molecular mechanisms underlying the resistance of BRAF V600E-mutant metastatic colorectal cancer to EGFR/BRAF inhibitors. *Ther. Adv. Med. Oncol.* **14**, (2022).
- 107. Mao, M. *et al.* Resistance to BRAF Inhibition in BRAF-Mutant Colon Cancer Can Be Overcome with PI3K Inhibition or Demethylating Agents. *Clin. Cancer Res.* **19**, 657–667 (2013).
- 108. Huijberts, S. C. F. A., Boelens, M. C., Bernards, R. & Opdam, F. L. Mutational profiles associated with resistance in patients with BRAFV600E mutant colorectal cancer treated with cetuximab and encorafenib +/- binimetinib or alpelisib. *Br. J. Cancer* **124**, 176–182 (2021).

- 109. Pálinkás, H. L. *et al.* Primary Founder Mutations in the PRKDC Gene Increase Tumor Mutation Load in Colorectal Cancer. *Int. J. Mol. Sci.* **23**, 633 (2022).
- 110. Chen, Y. *et al.* Role of PRKDC in cancer initiation, progression, and treatment. *Cancer Cell Int.* **21**, 563 (2021).
- 111. Loree, J. M. et al. Expanded Low Allele Frequency RAS and BRAF V600E Testing in Metastatic Colorectal Cancer as Predictive Biomarkers for Cetuximab in the Randomized CO.17 Trial. Clin. Cancer Res. 27, 52–59 (2021).
- 112. Benabdallah, N. S. *et al.* Aberrant gene activation in synovial sarcoma relies on SSX specificity and increased PRC1.1 stability. *Nat. Struct. Mol. Biol.* **30**, 1640–1652 (2023).
- 113. Godefroy, E. *et al.* Assessment of CD4+ T cells specific for the tumor antigen SSX-1 in cancerfree individuals. *Cancer Immunol. Immunother.* **56**, 1183–92 (2007).
- 114. Jerby-Arnon, L. *et al.* Opposing immune and genetic mechanisms shape oncogenic programs in synovial sarcoma. *Nat. Med.* **27**, 289–300 (2021).
- 115. Xie, N. et al. Neoantigens: promising targets for cancer therapy. Signal Transduct. Target. Ther. 8, 9 (2023).
- 116. Liu, L. *et al.* CCL15 Recruits Suppressive Monocytes to Facilitate Immune Escape and Disease Progression in Hepatocellular Carcinoma. *Hepatology* **69**, 143–159 (2019).
- 117. Xu, H. *et al.* New genetic and epigenetic insights into the chemokine system: the latest discoveries aiding progression toward precision medicine. *Cell. Mol. Immunol.* **20**, 739–776 (2023).
- 118. Trzpis, M., McLaughlin, P. M. J., de Leij, L. M. F. H. & Harmsen, M. C. Epithelial Cell Adhesion Molecule. *Am. J. Pathol.* **171**, 386–395 (2007).
- 119. Deep, G. & Agarwal, R. Targeting Tumor Microenvironment with Silibinin: Promise and Potential for a Translational Cancer Chemopreventive Strategy. *Curr. Cancer Drug Targets* **13**, 486–499 (2013).
- 120. Ding, F. The role of the ubiquitin-proteasome pathway in cancer development and treatment. *Front. Biosci.* **19**, 886 (2014).
- 121. Yeste-Velasco, M., Linder, M. E. & Lu, Y.-J. Protein S-palmitoylation and cancer. *Biochim. Biophys. Acta Rev. Cancer* **1856**, 107–120 (2015).
- 122. Park, S.-Y. *et al.* SUMOylation of TBL1 and TBLR1 promotes androgen-independent prostate cancer cell growth. *Oncotarget* **7**, 41110–41122 (2106).
- 123. Güre, A. O., Wei, I. J., Old, L. J. & Chen, Y. The SSX gene family: Characterization of 9 complete genes. *Int. J. Cancer* **101**, 448–453 (2002).
- 124. Itatani, Y. et al. The Role of Chemokines in Promoting Colorectal Cancer Invasion/Metastasis.

- Int. J. Mol. Sci. 17, (2016).
- 125. Xu, Z. & Kulp, D. W. Protein engineering and particulate display of B-cell epitopes to facilitate development of novel vaccines. *Curr. Opin. Immunol.* **59**, 49–56 (2019).
- 126. Sharma, P. & Allison, J. P. Immune Checkpoint Targeting in Cancer Therapy: Toward Combination Strategies with Curative Potential. *Cell* **161**, 205–214 (2015).
- 127. Gonzalez, H., Hagerling, C. & Werb, Z. Roles of the immune system in cancer: from tumor initiation to metastatic progression. *Genes Dev.* **32**, 1267–1284 (2018).
- 128. Lee, M. Y., Jeon, J. W., Sievers, C. & Allen, C. T. Antigen processing and presentation in cancer immunotherapy. *J. Immunother. Cancer* **8**, e001111 (2020).
- 129. Jiang, G.-M. *et al.* The relationship between autophagy and the immune system and its applications for tumor immunotherapy. *Mol. Cancer* **18**, 17 (2019).
- 130. Ruan, R. *et al.* Unleashing the potential of combining FGFR inhibitor and immune checkpoint blockade for FGF/FGFR signaling in tumor microenvironment. *Mol. Cancer* **22**, 60 (2023).
- 131. Phospholipase C-mediated cascade; FGFR2-Reactome. https://reactome.org/content/detail/R-HSA-5654221?utm\_source=chatgpt.com.
- 132. Guo, Q. *et al.* NF-κB in biology and targeted therapy: new insights and translational implications. *Signal Transduct. Target. Ther.* **9**, 53 (2024).
- 133. Mittal, S., Kamath, A., Joseph, A. & Rajala, M. PLCγ1-dependent invasion and migration of cells expressing NSCLC-associated EGFR mutants. *Int. J. Oncol.* (2020) doi:10.3892/ijo.2020.5112.
- 134. Balkwill, F. TNF-α in promotion and progression of cancer. *Cancer Metastasis Rev.* **25**, 409–416 (2006).
- 135. Hauser, A. S., Attwood, M. M., Rask-Andersen, M., Schiöth, H. B. & Gloriam, D. E. Trends in GPCR drug discovery: new agents, targets and indications. *Nat. Rev. Drug Discov.* 16, 829–842 (2017).
- 136. Turner, N. & Grose, R. Fibroblast growth factor signalling: from development to cancer. *Nat. Rev. Cancer* **10**, 116–129 (2010).

### 8. AKNOWLEDGMENTS

I would like to express my heartfelt gratitude to the Biosciences Laboratory of IRST in Meldola for providing me with the opportunity and resources to carry out my research. A special thanks to my PhD coordinator and tutor, Dr. Paola Ulivi, for her trust and continuous support throughout this journey. I am also deeply grateful to Professor Giovanna Cenacchi, who has guided me since my university years. My sincere appreciation goes to my colleague and dear friend Giorgia for everything she has taught me and for the invaluable help she has given me along the way.

Above all, my deepest gratitude goes to my husband Stefano and my son Alessandro, who are my greatest source of strength and motivation every single day. Their love, patience, and unwavering support have given me the energy and determination to pursue this path with passion and dedication.